Faculty of Pharmaceutical, Biomedical and Veterinary Sciences

Department of Pharmaceutical Sciences

Liver stage malaria

Investigating the interaction between the malaria circumsporozoite protein and host importin-α proteins

Laboratory of Medical Biochemistry

Promotor: prof. dr. ir. Yann Sterckx
Supervisors: ir. Rob Geens (main supervisor)
apr. Karen Claesen

Thesis submitted in partial fulfillment of the requirements for the Degree of Master in Drug Development

by Busra TURAN and Chaymae ABOUAZZA

Antwerp 2021

COPYRIGHT

Signed in Wilrijk, Belgium
Universiteitsplein 1, University of Antwerp

2020 - 2021

PROMOTER
Prof. dr. ir. Yann Sterckx

MAIN SUPERVISOR
Ir. Rob Geens

SUPERVISOR
Apr. Karen Claesen

AUTHORS
Busra Turan
Chaymae Abouazza

ACKNOWLEDGMENT

Although an end is part of the journey, new beginnings are necessary for a promising future. First and foremost, we would like to thank our promoter prof. dr. ir. Yann Sterckx. We are profoundly grateful to him for granting us this opportunity and enriching us with his knowledge. He is an exceptional lecturer but even a better promoter.

Secondly, our main supervisor ir. Rob Geens gave us invaluable help in every stage of our thesis. Even during late evenings at the lab, he was continuously available to assist us. We are convinced that our thesis would be impossible without his support. His compassionate suggestions, comments and compliments not only gave us a better sight of handling the writing but helped us mentally by boosting our confidence. We would also like to thank apr. Karen Claesen for the assistance with the cultivation of the cells and for her friendly smile.

We thank the University of Antwerp and the department of Pharmaceutical Sciences for making it possible, especially the staff members of the laboratory of Medical Biochemistry as highlighted. They are a tight team, making the laboratory a pleasant and educative environment to work in.

I would like to thank my father and my sisters for being there for me in both good and bad times. I owe you everything and I cannot thank you enough. My friend and roommate Nisa Erdal always supported me and provided a sympathetic ear. I also want to thank my friends Gulnihal Aydin, Ahlam Rozaine, Seren Bilmis and Beyza Batmaz for doing their best to help me although this topic is beyond their scope of expertise.

Busra Turan

First of all, I would like to thank my parents and my younger brother for their unwavering support and belief in me. They have always been by my side and helped me through all the difficult times. Without their tremendous understanding and encouragement, I would not have come this far. I am also deeply grateful for my friends who always lent me a listening ear and for their efforts to uplift my mood.

Chaymae Abouazza

Last but not least, we want to thank each other. Helping one another for almost five years to get through an academic career and for being a good friend.

'' Nothing in life is to be feared,

it is only to be understood.

Now is the time to understand more,

so that we may fear less.''

Marie Curie

CONTENTS

ABBREVIATIONS

ACT	artemisinin-based combination therapy
CBB	Coomassie Brilliant Blue
CSP	circumsporozoite protein
CV	column volume
DMEM	Dulbecco's Modified Eagle's Medium
DMSO	dimethylsulfoxide
EMA	European Medicines Agency
FBS	fetal bovin serum
FL	full-length
GPI	glucose phosphate isomerase
HAC	heparin affinity chromatography
HS-HSPGs	highly sulfated heparan sulfate proteoglycans
HSPGs	heparan sulfate proteoglycans
IMAC	immobilized metal affinity chromatography
MBs	magnetic beads
MRZs	merozoites
MQ	Milli-Q water
Nbs	nanobodies
NLS	nuclear localization signal
P. berghei	*Plasmodium berghei*
***Pbe*CSP$_{FL}$**	*Plasmodium berghei* circumsporozoite protein full-length
PBS	phosphate-buffered saline
PEXEL	*Plasmodium* export element
P. falciparum	*Plasmodium falciparum*
***Pfa*CSP$_{FL}$**	*Plasmodium falciparum* circumsporozoite protein full-length

PV	parasitophorous vacuole
P. yoelii	*Plasmodium yoelii*
PTEX	*Plasmodium* translocon of exported proteins
PVM	parasitophorous vacuolar membrane
SEC	size exclusion chromatography
SDS-PAGE	sodium dodecyl sulfate polyacrylamide gel electrophoresis
SPZs	sporozoites
TRAP	thrombospondin-related anonymous protein
TRIS	tromethamine
TSR	thrombospondin-like type I repeat
WB	western blot

CHAPTER I

INTRODUCTION

Malaria is a mosquito-borne infectious disease and considered as one of the 'Big Four' deadliest human-infectious diseases (1). According to the World Health Organization, more than 229 million clinical cases and 409 million deaths were reported in 2019. Children under the age of five accounted for 67% of all malaria deaths worldwide. Parasites of the *Plasmodium* genus are responsible for the disease, of which *P. falciparum* is the most virulent human-infective strain (2).

The transmission of the parasite to the human host takes place during a blood meal by the *Anopheles* mosquito, the vector. This leads to the introduction of the parasite into the human body under its sporozoite (SPZ) form. A malaria infection consists of two stages: the liver and the blood stage. After being bitten by an *Anopheles* mosquito, SPZs are injected in the skin and reach the liver through the bloodstream. Those SPZs then infect the hepatocytes, transform into merozoites (MRZs) and are released from the liver cell into the bloodstream (3, 4).

Once the infection reaches the blood phase, the first signs of the disease may start to show with fever attacks (so-called "paroxysms") as the most remarkable symptom. Nausea, body aches and headaches are also other symptoms that typically occur. Leaving malaria untreated or poorly treated can lead to severe complications with a potentially fatal outcome (3, 4). Acquired resistance against antimalarial drugs has further increased the need for an effective malaria vaccine and the amelioration of the existing antimalarial drugs. Because the SPZs play a prominent role in the infection, they might be an interesting target for further research (2, 5).

During its life cycle, the parasite produces a myriad of stage-specific surface proteins. The variety of those surface proteins make the battle against this parasite even more complex, but on the other hand they also offer a diversity of opportunities in the development of new antimalarials. The reason why

those SPZ surface proteins are so important, is because by eliminating SPZs both the disease and the transmission can be prevented (6).

One of those SPZ surface proteins, and the most prominent one, is the circumsporozoite protein (CSP) whose structure-function relationship remains poorly understood, despite decades of research. CSP has many functions, making it very thought-provoking and research can clear up the mechanisms in the liver stage. It plays a central role in the immunobiology of the malaria parasite in both the mosquito and vertebrate hosts. In the latter it is known that CSP plays a prominent role in the SPZ's recognition and afterwards invasion of the hepatocyte. Once inside the hepatocyte, CSP has been proposed to be translocated to the cytoplasm as an effector protein to manipulate the host environment. It is speculated that in the cytoplasm, CSP competes with transcription factors by interacting with members of the importin-α family. This may lead to the dampening of the inflammatory responses, resulting in the survival and further development of the parasite during the liver stage (5).

By investigating this possible interaction of CSP and the importin-α proteins, the aim is to discover more about the structure and mechanism of CSP and to validate the known information.

CHAPTER II

LITERATURE REVIEW

2.1 MALARIA: A GLOBAL HEALTH BURDEN

Malaria is a vector-borne infectious disease caused by *Plasmodium* parasites that are transmitted by female *Anopheles* mosquitoes. It is endemic in tropical and subtropical areas, where the mosquito and the parasite have the ideal environment to survive due to the temperature and humidity (Figure 2.1) (3).

The most dominant human-infective *Plasmodium* species are *P. vivax* and *P. falciparum*, of which the latter is responsible for the deadliest form of malaria. In 2019, over 220 million clinical cases and more than 400 million deaths were reported, with children aged under five years being the most vulnerable population. More than 95% of those cases globally occurred in 26 countries, mainly in the Sub-Saharan region (51%) (2).

It is crucial to know more and to validate the known information. The survival of the *Anopheles* mosquito and the parasites are both linked to the climatic conditions. In the 1970s malaria was eradicated from Europe (7). However due to the climate change, the return of the disease is plausible as was recently evidenced by mysterious cases in Italy and Belgium in 2017 and 2020, respectively (8) and (9). Considering that malaria is already causing so much trouble globally and the ongoing climate change, basic research on this topic is crucial (7).

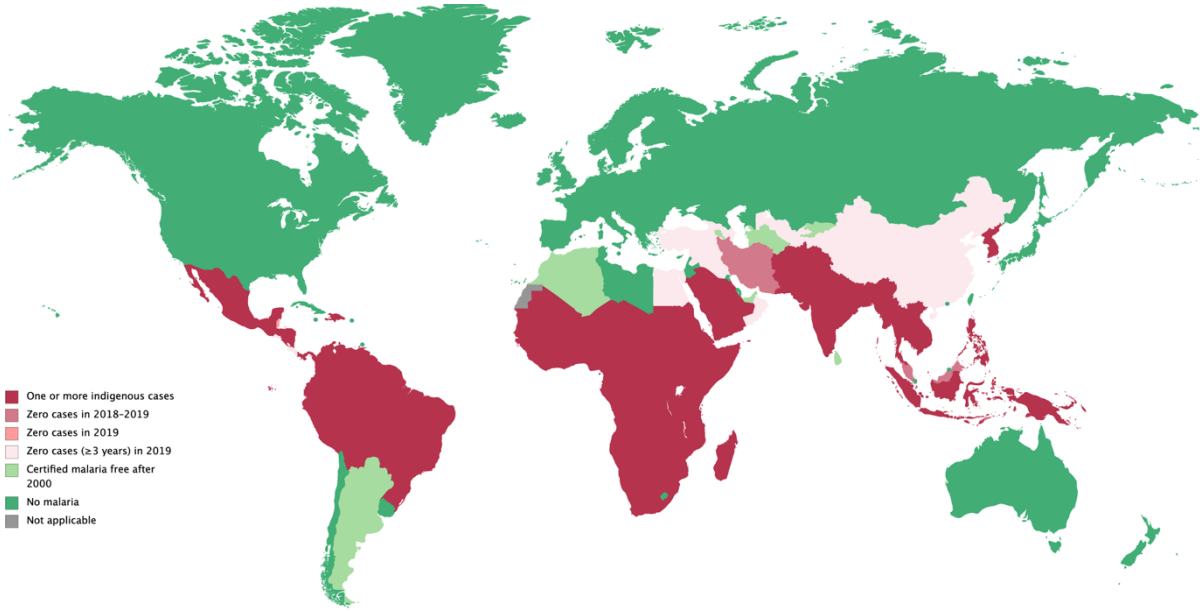

Figure 2.1 **MALARIA WORLD MAP.** This world map shows the distribution of malaria cases around the globe. Figure adapted from ref (2).

2.2 THE BIOLOGY AND PATHOLOGY OF THE *PLASMODIUM* PARASITE

2.2.1 The life cycle of the parasite in the human body is an organized mechanism

A malaria-infected female *Anopheles* mosquito injects the parasites into the skin of the human host during a blood meal (Figure 2.2). The first life form of the parasite is called the sporozoite (SPZ). The SPZs have a gliding[1] motility that ensures that they reach the liver cells and invade them. The journey from the skin to the liver is called the 'pre-erythrocytic phase' and is clinically silent (10).

Inside the hepatocyte, one SPZ develops into thousands of merozoites (MRZs), the second life form of the parasite. Eventually, the MRZs are released into the blood circulation, where they initiate an asexual reproduction cycle consisting of the following four steps: i) invasion of erythrocytes, ii) remodeling of the infected erythrocyte to ensure the survival of the parasite, iii) maturation of the parasite in the erythrocyte, and iv) release of the newly formed MRZs. The cycle can now start again by invading other erythrocytes (10).

A small subset of parasites may differentiate into male and female gametocytes which in turn lead to the sexual reproduction cycle inside the next mosquitoes feeding off the infected human (10) (Figure 2.2).

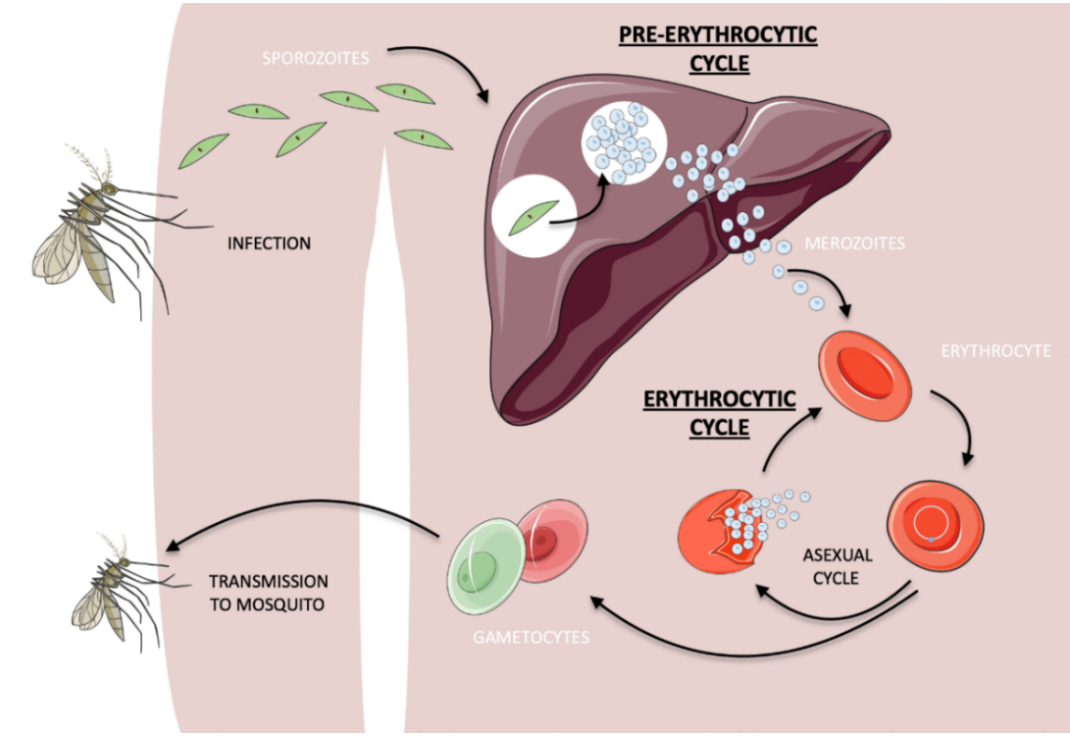

Figure 2.2 **SCHEMATIC REPRESENTATION OF THE *PLASMODIUM* LIFE CYCLE**. The life cycle of malaria with the female *Anopheles* mosquito as host and vector of the parasite and the human body as the host.

[1] Substrate-dependent movement where the SPZ maintains its shape (30, 32)

2.2.2 The aftermath of an infection by a malaria parasite

As mentioned before, the notorious malaria pathology is caused by the blood stage or erythrocytic stage of the infection, while the liver or pre-erythrocytic stage is clinically silent. Symptoms occur after seven days to a month, are periodic and most commonly exist of fever attacks, nausea and vomiting, malaises, headaches, chills, sweats and body aches (3).

The fever attacks and rigors occur after red blood cells rupture and MRZs are released, infecting other blood cells. Those attacks are typically periodic and can reoccur every three or four days, depending on the malaria species (3, 11).

Untreated or undertreated malaria can lead to severe cases. In general, there are three syndromes that are known to have a very high mortality: severe anemia, cerebral malaria and respiratory distress (3, 12). Anemia is a prominent consequence of malaria following the hemolysis of the red blood cells. This loss of red blood cells can also result in jaundice. Moreover, infected red blood cells attach to the vascular endothelium and in specific cases, this may result in cerebral or placental malaria (3, 11, 13). Acute respiratory distress syndrome is another manifestation of severe malaria as a result of systemic inflammation and metabolic acidosis (3, 14).

2.2.3 The battle against malaria requires a multidisciplinary strategy

Malaria is a global health burden which, given the complexity of the parasite life cycle, requires a multifaceted strategy to prevent, control, cure and eventually eradicate the disease. This is not self-evident and requires several tools: vector control, diagnosis, treatment and vaccination (15).

VECTOR CONTROL. The first and most widely employed tool is vector control, which has proven itself to be highly effective over history. By denying the female *Anopheles* mosquito a blood meal, both disease and further transmission can be avoided. This method was used in Northern America and Europe and resulted in the elimination of malaria. The two major methods involved are pyrethroid insecticide-treated nets (ITNs) and indoor residual spraying (15-17). An uprising problem is the mosquito resistance against insecticides, but research has showed that applying antimalarials on those nets may be a hopeful solution to halt transmission (15, 18, 19).

DIAGNOSIS. There are three effective ways to detect whether a person is infected or not, namely microscopy, rapid diagnostic tests and *Plasmodium* species-specific PCR. An accurate diagnosis then leads to the next step or third tool: the treatment of malaria (3, 20).

TREATMENT. Because malaria can have a fatal outcome, an immediate and adequate treatment is crucial. The kind of treatment that can be used depends on, not only the state of the patient, but also on the parasite species and the geographical region (3). In case of uncomplicated malaria, chloroquine can be used, but because of the growing resistance against this drug, artemisinin-based combination therapy is a better and more effective option. However, in some area's artemisinin-resistant *P. falciparum* cases have been noticed. This growing problem of drug-resistance is a reason to consider developing novel anti-malaria drugs instead of ameliorating existing drugs and is also a driving force for finding new ways to combat the malaria disease, for example a vaccine (2, 11, 21-23).

A VACCINE. There are several vaccines in development, targeting different life cycle stages of the parasite: the pre-erythrocytic stage (SPZs), asexual blood stage (MRZs) and the sexual blood stage (gametocytes) (24, 25). Vaccines with the MRZs as target, can prevent the manifestation of the disease. This is not the case for the transmission blocking vaccines, targeting the sexual stage, because they can only block the transmission but have no effect on the infection or the clinical symptoms (24, 25).

An example of a vaccine targeting the pre-erythrocytic stage is the RTS, S/AS01 vaccine, which is a CSP subunit vaccine and thus targets the SPZs before entering the hepatocytes. This vaccine is very interesting because it does not only block the infection and disease, but also further transmission However, this is only a subunit vaccine and not a whole SPZ vaccine, which can restrict the efficacy against variants. Therefore, it may be more interesting to develop whole SPZ or full length CSP vaccines (6, 26-28). Another interesting strategy is, instead of targeting a specific stage of the parasite, to target multiple life stages (24, 25).

2.3 THE JOURNEY OF THE SPOROZOITE: 'A LONG AND WINDING ROAD'

The remarkable journey of the *Plasmodium* SPZs in its mammalian host begins in the skin and ends up in the liver (29). Mature SPZs are slender shaped and motile cells. Interaction between different SPZ surface proteins such as thrombospondin-related anonymous protein (TRAP) and host receptors are crucial for the 'gliding motility' of these cells (30, 31).

At the apical end of the apicomplexan SPZs, three specialized secretory organelles are localized (Figure 2.3). Proteins stored in the micronemes, rhoptries and dense granules are respectively important for the cell adhesion and motility, for the invasion and formation of the parasitophorous vacuole (PV) and for modification of the host cell during invasion (30, 31).

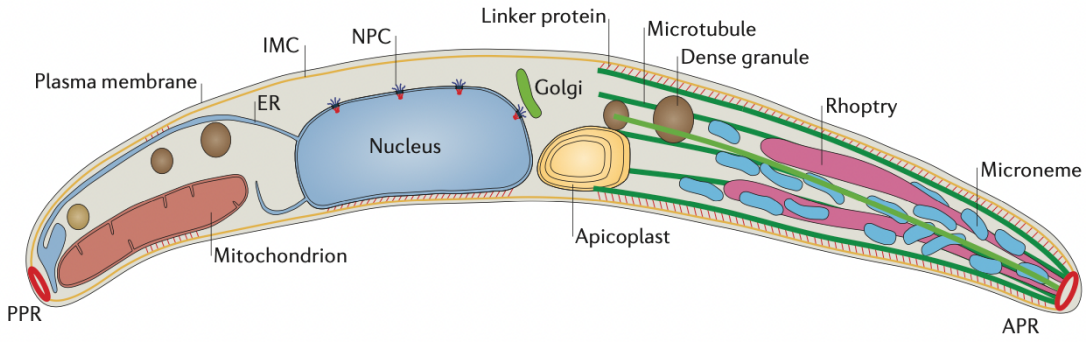

Figure 2.3 **STRUCTURE OF THE SPOROZOITE**. The secretory organelles: dense granules (brown), rhoptries (pink) and micronemes (blue) are localized at the apical end. Figure reprinted from ref (30).

INOCULATION INTO THE SKIN. After a bite by an infected mosquito, a small number (50-100) of SPZs are injected directly into the skin. The gliding motility ensures that these SPZs can travel through the skin with three possible destinations: I) reaching the bloodstream to eventually end up in the liver; II) staying in the skin; and III) draining by lymphatic nodes which results in elimination by macrophages and dendritic cells (30, 32).

THE JOURNEY TO THE LIVER. SPZs recognize different cell types based on the sulfation level of their heparan sulfated proteoglycans (HSPGs) [2] (30, 33). This is based on the specific interaction between the SPZ's major surface antigen (the circumsporozoite protein, CSP) and highly sulfated HSPGs (HS-HSPGs), which are typically presented on the surface of liver cells (30). During their migratory mode, *Plasmodium* SPZs can also traverse cells with low-sulfated HSPGs (LS-HSPGs) on their surface but do not infect those cells productively (29, 32). Due to fenestration in the blood vessels,

[2] A family of glycoproteins present on the surface of most mammalian cells (30).

the HS-HSPGs can be recognized by SPZ (Figure 2.4). The motility decreases due to this interaction, which results in the arrest of the SPZs (30, 34).

INVASION OF THE HEPATOCYTES. Prior to invasion of the hepatocytes, SPZs need to cross the sinusoidal barrier, which consists of three types of liver cells: Kupffer cells[3], endothelial cells and stellate cells[4] (Figure 2.4). The SPZ can rely on five different pathways, but traversing Kupffer cells via the formation of a vacuole, is the best studied pathway (30, 34). After crossing the sinusoidal barrier, SPZs reach the hepatocytes.

However, the switch from the 'migratory mode' to the 'invasion mode' of the SPZs is a progressive process. Migration of SPZs through different hepatocytes leads to the exposure of parasitophorous membrane proteins, such as TRAP and apical membrane antigen 1 (AMA1) by the secretory organelles localized at the apical end of the SPZs. These proteins form an 'apical cap' to enlarge the contact between the hepatocytes and SPZs, which is required for invasion (34). The contact with hepatocytes also triggers the proteolytic cleavage of the CSP by a cysteine protease, which is essential for the activation of the invasion mode (30, 35). When SPZs invade a final hepatocyte, a PV is formed, providing the necessary nutrients and ensuring the survival of the parasite (30, 33, 34).

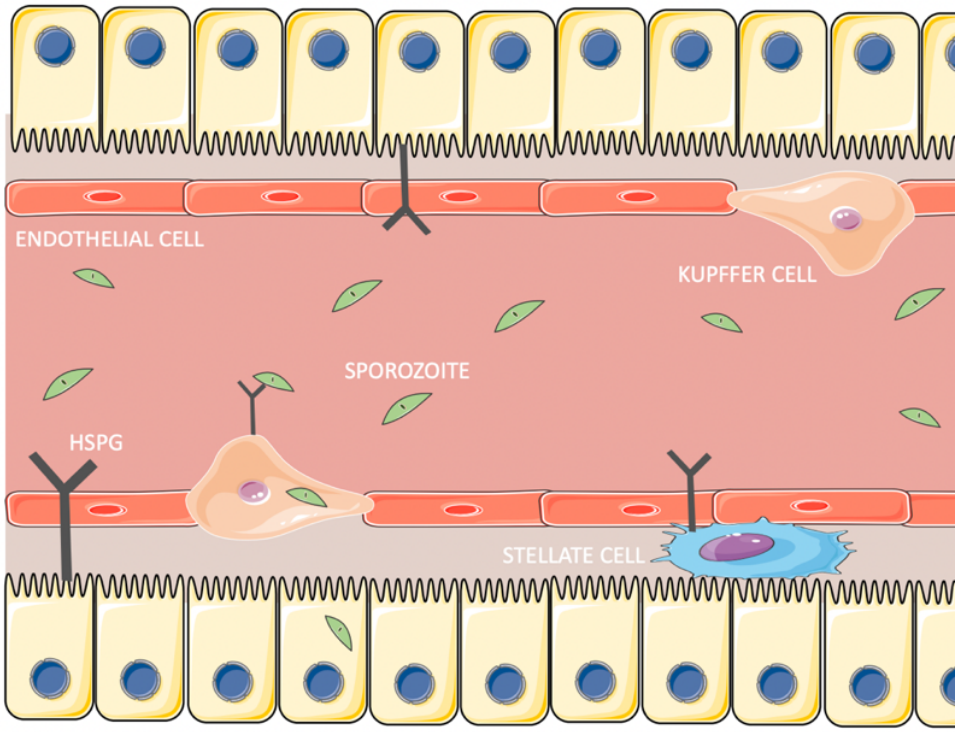

Figure 2.4 **CROSSING THE LIVER SINUSOIDS**. The SPZs (green) interact with HS-HSPG (dark grey), cross the endothelial sinusoidal layer (orange) and reach the hepatocytes (yellow).

[3] A macrophage localized in liver between the lumen and sinusoids.
[4] A star-like shaped liver cell localized between hepatocytes and endothelial cells.

2.4 THE CIRCUMSPOROZOITE PROTEIN IS THE SPORZOITE'S KEY PLAYER

2.4.1 The architecture of the circumsporozoite protein

CSP has a molecular mass between 32 and 48 kDa, depending on the *Plasmodium* species and isolate (36). Despite differences in amino acid composition, all CSPs have the same modular build-up composed of three main domains: a N-terminal domain with a signal peptide, a central repeat region and a C-terminal domain with a glycosylphosphatidylinositol (GPI) anchor to attach CSP to the surface of the parasite (37) (Figure 2.5). The N-terminal junction forms a connection between the N-terminal domain and the central repeat region. The C-terminal junction connects the central repeat region with the C terminal domain (38, 39).

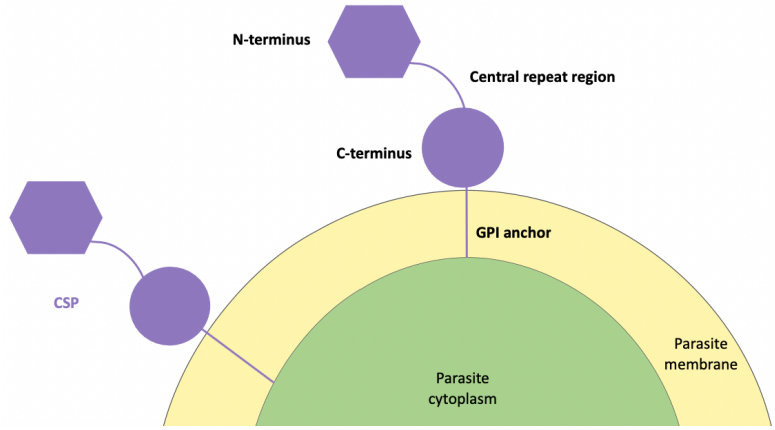

Figure 2.5 **CSP IS THE MAIN SURFACE PROTEIN OF THE PARASITE.** Schematic representation of CSP on the sporozoite's surface.

N-TERMINAL DOMAIN. The N-terminal domain of CSP contains several conserved regions. The stretch of amino acids in the N-terminal domain composed of KLKQP is called Region I. This highly conserved region plays a crucial role during hepatocyte invasion (5, 35). Depending on the *Plasmodium* species, one or two *Plasmodium* export element (PEXEL) motifs are also present in this domain, which might be involved in CSP's intracellular effector function (5, 36). However, the structure of the N-terminus remains enigmatic.

CENTRAL REPEAT REGION. The linker repeat region contains tandem repeats of which the composition and number depend on the *Plasmodium* species and isolate (36). The tandem repeats in *P. falciparum* contain the tetrapeptide: Asn-Ala-Asn-Pro (NANP). This region is interrupted with four copies of another tetrapeptide: Asn-Val-Asp-Pro (NVDP) (37). CSP has been observed to adopt various conformations due to the highly flexible and dynamic character of the linker, which gives the protein features of an intrinsically disordered protein (40). The elongated and flexible NANP-structure shows a stem-like (elongated helical) structure, giving CSP an overall rod-like shape (38).

C-TERMINAL DOMAIN. The C-terminal domain is most probably the only CSP domain with a well-defined globular fold (Figure 2.6). It is composed of Region III, the highly conserved Region II+ and the nuclear localization signal (NLS) motif. The C-terminal domain adopts an αTSR fold which consists of an α-helix on the N-terminal side, a typical thrombospondin-like type I repeat (TSR) fold and a CSP-flap (39). Region III forms the α-helix and contains a polymorphic Th2R region. The α-helix lies perpendicular to the TSR-like domain which consists of three antiparallel strands of which two are β-strands (39, 41). The two β-strands are connected by a flexible fold called the CSP-flap (39) (Figure 2.6B). This CSP-flap contains a polymorphic Th3R region and the NLS motif. The NLS motif is believed to play a pivotal role in the transport of CSP by the importin-α proteins to the nucleus of the liver cells (5, 39).

During the migratory mode, the C-terminal region of CSP is shielded by the N-terminal domain, which results in protection against possible attacks from the immune system. This shield is only removed during hepatocyte invasion when the migratory mode is switched for the invasion mode due to conformational changes. The N-terminus is cleaved proteolytically, leaving the C-terminus unprotected. Thus, the conformation of CSP changes from an open or non-adhesive state to a collapsed or adhesive state which emphasizes the role of the C-terminus in the hepatocyte's invasion (35, 41, 42). This flexibility of CSP may be the factor that helps with the SPZ motility and hepatocyte invasion (41-43).

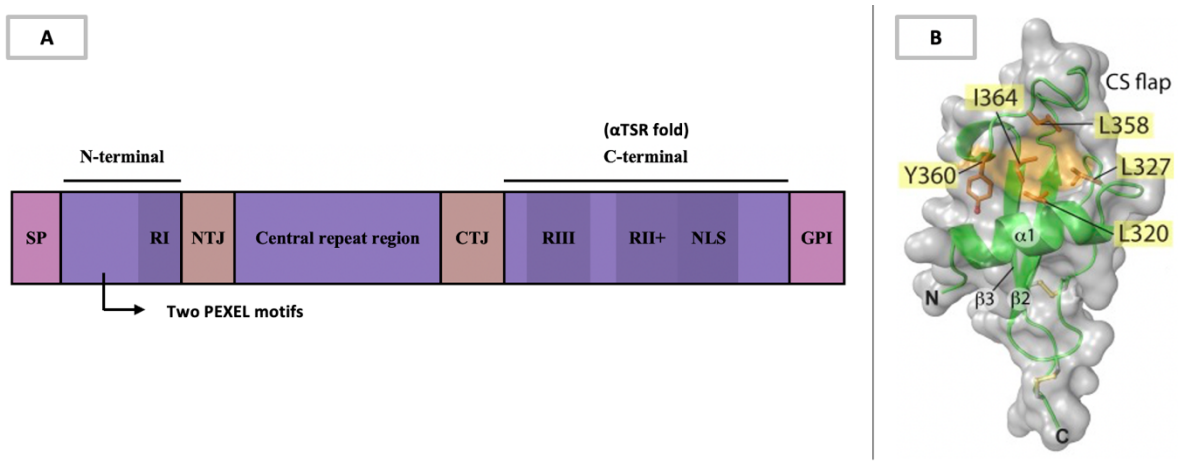

Figure 2.6 **THE GENERAL ARCHITECTURE OF CSP.** (A) SP = signal peptide, RI = Region I, NTJ = N-terminal junction, CTJ = C-terminal junction, RIII = Region III, RII+ = Region II+, NLS = the nuclear localization signal, GPI = glycosylphosphatidylinositol anchor. (B) Crystal structure of the α-TSR domain. Figure reprinted from ref. (39).

2.4.2 The functions of the circumsporozoite protein

CSP plays a central role in the immunobiology of the malaria parasite, not only in the vertebrate host but also in the insect host (44). However, the functions in the latter are not relevant for this thesis and will not be further discussed here. The first proposed function of CSP inside the vertebrate host is to protect the SPZ during its migration through the skin by forming a shield at the surface (45). Secondly it is the main antigen that interacts with the humoral immune system of the host (46). Thirdly, after reaching the liver cells, CSP is essential for hepatocyte invasion by interacting with HS-HSPGs, typically presented by those hepatic cells (47, 48). Finally, once settled inside the infected liver cell, evidence has suggested that the parasite translocates CSP to the host cell's cytoplasm (5, 45, 48-50). It is believed that CSP has an intracellular effector function. CSP possibly competes with the transport of transcription factors to the nucleus resulting in the dampening of the inflammatory responses to ensure parasite survival (5, 45, 48, 49) (Figure 2.7).

2.4.3 The circumsporozoite protein is believed to have an intracellular effector function during liver stage malaria

In this thesis, the focus lies on the liver stage and more specifically on the possible intracellular effector function of CSP inside the infected hepatocyte. First, it is important to mention that the liver stadium is clinically silent. This is interesting, considering that a parasite resides inside the liver cell and takes up more than a half of the volume, causing enormous stress. Moreover, the fact that no apoptotic markers are observed, suggests that cell death is suppressed somehow by the parasite (51). This all indicates that the parasite most likely manipulates its environment to promote its survival inside the infected host cell, as death of the latter would imply a halt in the parasite's life cycle. In case of the MRZs, which infect red blood cells and reside in a PV as well, it is known that the parasite translocates proteins from the parasite to the host cytoplasm through the PV membrane (PVM) to remodel the host cell (52). Many of these proteins contain a *Plasmodium* export element (PEXEL) motif, composed of the semi-conserved pentapeptide RxLxE/Q/D (53, 54). The export of PEXEL-positive proteins is mediated by the *Plasmodium* translocon of exported proteins (PTEX), a complex of various proteins located in the PVM (55-57). Interestingly, CSP possesses one or two (depending on the species) functional PEXEL motifs in its N-terminal domain, suggesting that PTEX-mediated export is an event that does not only occur during the blood stage, but might also play a role during the liver stage (5) (Figure 2.7). Whether or not PTEX-mediated export of parasite effector proteins occurs inside the infected hepatocyte remains an open question in the field of SPZ biology.

Inside the hepatocyte's cytoplasm, CSP has been proposed to interact with ribosomes, possibly interfering with the host cell's protein synthesis machinery (50). Besides interacting with ribosomes, CSP has been shown to be translocated to the nucleus of the liver cells (5) (Figure 2.7). This translocation event is proposed to be mediated by members of the importin-α protein family, since CSP possess a nuclear localization signal (NLS). Importin-α proteins typically recognize the cargo they must transport by their NLS. In the case of CSP, the NLS is located in the CSP-loop of the αTSR domain, where it is freely available and exposed for interaction with importins. A study reported that each member of the importin-α protein family has a different strength in interaction with CSP, with importin-α3 as the strongest interaction partner (5). The precise biological function of CSP in the nucleus remains unclear, but it is presumed that CSP competes with host transcription factors (particularly NFκB) for interaction with importin-α proteins (5, 58). This may lead to a diminution of the inflammatory response and gives the chance to the parasite to fully develop by forming an ideal, protective niche (5).

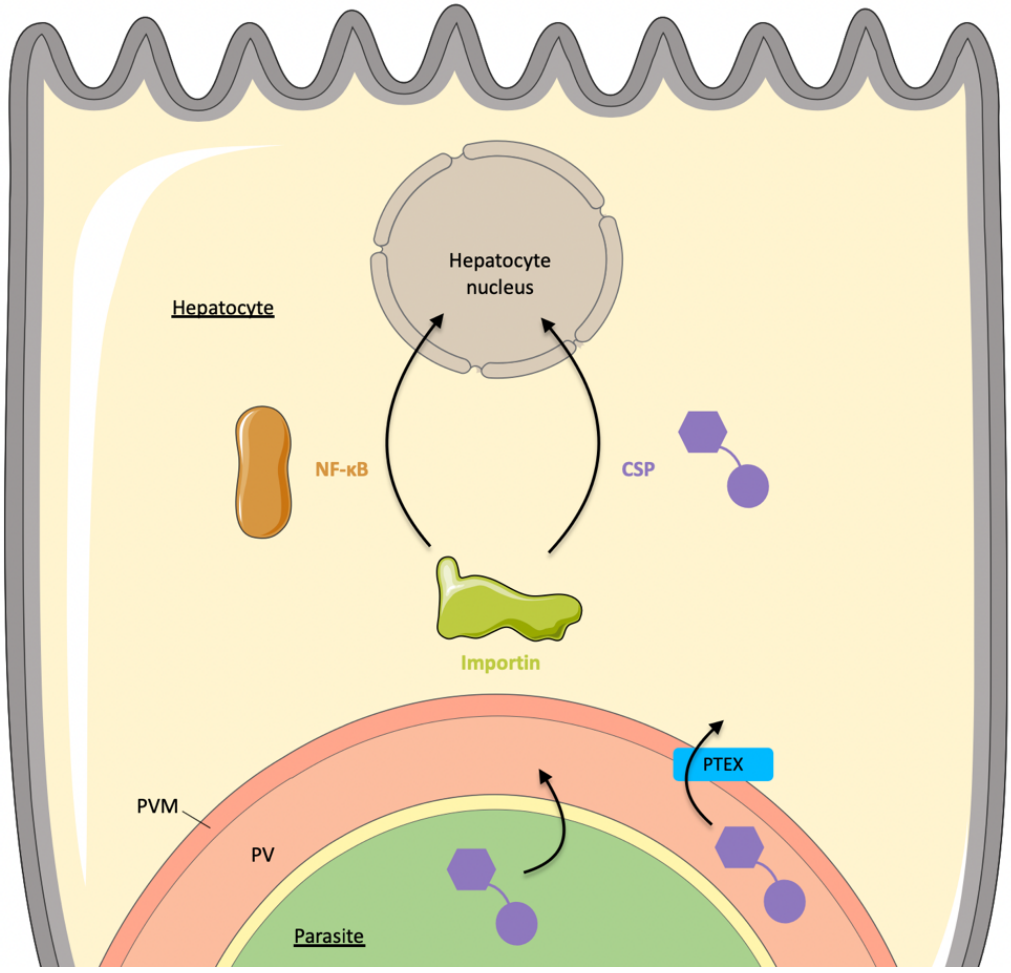

Figure 2.7 **CSP PLAYS A ROLE IN THE SURVIVAL OF THE PARASITE INSIDE THE LIVER CELL.** CSP is transported from the PV to the cytoplasm by PTEX. In the cytoplasm it is believed to interact with the importin-α proteins. According to Singh et al., 2007, CSP may be transported to the nucleus by the importin-α proteins, resulting in a competition with NFκB to dampen inflammatory responses (5).

CHAPTER III

AIMS OF THIS THESIS

While it has been proposed that the CSPs from the rodent-infective *Plasmodium* species *P. yoelii* (*Pyo*CSP) and *P. berghei* (*Pbe*CSP) are translocated to the cytoplasm and nucleus of infected host hepatocytes, the exact mechanisms of translocation remain elusive and have only been described in a single paper (5). It has been described that *Pyo*CSP interacts with members of the importin-α protein family by *in-vitro* pull-down assays with recombinantly produced proteins (5, 59). However, the biophysical and structural aspects of this interaction have not yet been investigated, nor has this interaction been validated for CSP from other *Plasmodium* species. Investigating the above-mentioned aspects of the possible intracellular effector function of CSP during liver stage malaria may provide new insight in the complex immunobiology of the parasite.

This master thesis contributes to the ongoing investigation on the interaction between CSP and members of the importin-α protein family and had the following aims:

- Recombinant production of full-length *Pfa*CSP and *Pbe*CSP (*Pfa*CSP_{FL} and *Pbe*CSP_{FL}, respectively) in *E. coli*
- Purification of *Pfa*CSP_{FL} and *Pbe*CSP_{FL} via the following chromatographic methods:
  - Immobilized metal affinity chromatography (IMAC)
  - Size-exclusion chromatography (SEC)
  - Heparin affinity chromatography (HAC)
- Cultivation of Hepa1-6 and HepG2 cells and preparation of cell lysates
- Investigation of the interaction between *Pfa*CSP_{FL} and *Pbe*CSP_{FL} and members of the importin-α protein family by pull-down assay

CHAPTER IV

MATERIALS AND METHODS

4.1 MATERIALS

CELL CULTURE	
Cells	HepG2 (Silvie lab) Hepa1-6 (Silvie lab)
Complete growth medium	Dulbecco's Modified Eagle's Medium (DMEM) (Gibco) 1% penicillin 10% fetal bovine serum (FBS) heat inactivated (HI) Store at -20°C
Lysis buffer	10mM Tris 150 mM NaCl 0.02% NaN_3 1% Triton X-100 1x tablet of a Protease Inhibitor Cocktail Tablets (Roche, COMPLETE tablets)
Enzyme	1X TrypLE Express (Gibco)
PROTEIN PRODUCTION	
Vector	pET21b plasmid

Bacterial growth media	
Super optimal broth with catabolite repression (SOC) medium	2.00% Tryptone 0.50% Yeast extract 10 mM NaCl 2.5 mM KCl 0.40% Glucose 10 mM $MgSO_4$ 10 mM $MgCl_2$ Autoclave
LB-agar/Glucose/Ampicillin plates	2.50% LB Miller Broth (high salt) 1.50% NaCl
2x Tryptone Yeast extract, 2xTY medium	1.60% Tryptone 1.00% Yeast extract 0.50% NaCl pH 8.0 Autoclave
Antibiotic	
1000x Ampicillin stock solution	100mg/mL in 70% Ethanol Filter (0.22 μm) Store at -20°C
Molecular reagents	
1000x Isopropyl β-D-1-thiogalactopyranoside (IPTG) stock solution	1 M IPTG Filter (0.22 μm) Store at -20°C
1000x protease inhibition mix (PIM)	2 mM Leuptin 125 mM AEBSF 100 mM EDTA Filter (0.22 μm) Store at -20°C
Stock solutions	
20% Glucose stock solution	20% D-glucose Autoclave

50% Glycerol stock solution	50% Glycerol Autoclave
Buffer	
Lysis buffer A	50 mM Tris 500 mM NaCl 20 mM Imidazole 1x PIM pH 8.0 Filter (0.45 µm) Degas
PROTEIN PURIFICATION	
Buffers	
Buffer A	Idem lysis buffer A
Buffer B	50 mM Tris 500 mM NaCl 1 M Imidazole 1x PIM pH 8.0 Filter (0.45 µm) Degas
Buffer C	50 mM Tris 1x PIM pH 8.0 Filter (0.45 µm) Degas
Buffer D	50 mM Tris 1 M NaCl 1x PIM pH 8.0 Filter (0.22 or 0.45 µm) Degas
Columns	

Immobilized metal affinity chromatography (IMAC)	5 mL HisTrap HP (GE Healthcare)
Size-exclusion chromatography (SEC)	HiLoad 16/60 Superdex200 pg (GE Healthcare)
Heparin affinity chromatography (HAC)	1 mL HiTrap Heparin HP (GE Healthcare)
SDS-PAGE & WESTERN BLOT SOLUTIONS	
Protein marker	Precision plus protein dual color standard (Bio-Rad)
Buffers	
Phosphate buffered saline (PBS)	137 mM NaCl 2.7 mM KCl 10 mM Na_2HPO_4 1.8 mM KH_2PO_4 pH 7.5
Blocking buffer	5% skimmed milk powder In PBS
Washing buffer (PBST)	0.1% Tween20 In PBS
20x 2-(N-morpholino) ethanesulfonic acid (MES) electrophoresis buffer	1M MES 1M Tris 2% SDS 20 mM EDTA
Transfer buffer	0.2 mM Glycine 25 mM Tris 20% Methanol
Antibodies	
Primary antibodies	Mouse anti-His mAb (Bio-Rad, clone AD1.1.10) Mouse anti-importin-α mAb (Sigma, clone IM-75)
Secondary antibody	Goat anti-mouse (Sigma, clone A4416)
Developing substrate	
Kits	Pierce™ CN/DAB Substrate Kit (Thermo Scientific)

	SuperSignal West Femto Maximum Sensitivity Substrate (Thermo Scientific)
PULL-DOWN ASSAYS	
Quickpick IMAC kit (Bio-Nobile)	
Magnetic Beads	IMAC magnetic particles Phosphate buffer (pH 7.0) NaCl Tween20 0.02% NaN_3
Regeneration Buffer	Aqueous $NiSO_4$ solution Tween20 0.02% NaN_3
Wash buffer 1	Phosphate buffer (pH 7.0) 250 mM NaCl Tween20 0.02% NaN_3
Wash buffer 2	Phosphate buffer (pH 7.0) 250 mM NaCl 20 mM Imidazole 0.02% NaN_3
Elution Buffer	20 mM Tris-HCI (pH 8.0) 250 mM NaCl 300 mM Imidazole 0.05% Tween20 0.02% NaN_3
DEVICES	
Centrifuge	Multifuge 35-R Heraeus
Vortex	Lab-Line Instruments inc. Super-mixer
Centrifugal filter devices	10K Amicon Ultra-0.5 mL Centrifugal Filters (Merck)

4.2 METHODS

4.2.1 Cell culture

CELL LINES. Hepa1-6 and HepG2 cells were cultured for the experiments further described in this master thesis. The Hepa1-6 cell line is a murine liver cell line, while the HepG2 cell line is a human hepatocyte cell line. The cells were grown in cell culture T-flasks (Greiner Bio-One) and maintained in a humidified incubator at 37°C under 5% CO_2. Both cell lines were kindly provided by dr. Olivier Silvie (INSERM, Paris, France).

CELL THAWING. The cells were stored in liquid nitrogen with dimethylsulfoxide (DMSO) as cryoprotectant. To thaw the cells, the cryotube was shortly placed in a water bath at 37°C. The thawed cells were then transferred to a tube and complete growth medium was added. This suspension was then centrifuged for 5 minutes at 125*x*g. Subsequently, the supernatant was removed, and the pellet was resuspended in 10 mL growth medium, whereafter, the cell suspension was transferred to a T25 flask and incubated at 37°C and 5% CO_2.

CELL SUBCULTIVATION. When 80% confluency was reached, the cells were subcultivated. To do so, the growth medium was removed. This caused no issue because the cells are adherent and stay behind in the flask. The cells in the flask were then washed with pre-heated phosphate-buffered saline (PBS).

After discarding the PBS from the flask, 1X TrypLE Express was added to disassociate the adherent cells, whereafter the flask was incubated for 5 minutes at 37°C. To make sure that the dissociation was completed, an inverted microscope was used to look at the cells. The cells are now clearly moving and fleeting instead of adhering to the wand. In a next step the 1X TrypLE Express was neutralized by adding growth medium, which contains FBS that inhibits trypsin.

The content of the flask was transferred to a tube and centrifuged for 5 minutes at 125xg. Then, the supernatant was removed, and the pellet was resuspended in pre-heated growth medium. Afterwards, the suspension was divided into new flasks. The recommended subcultivation ratio is 1:4 to 1:6 for HepG2 cells and 1:3 to 1:8 for Hepa1-6 cells. If needed, growth medium can be added to the flasks to reach the end volume. The amount of reagent required during the cultivation, differs depending on the size of the flask (Table 4.1).

Table 4.1 **THE AMOUNT (ML) OF PRODUCT THAT WAS USED, DEPENDING ON THE SIZE OF THE FLASKS.**

Flask (cm^2)	PBS (mL)	1X TrypLE Express (mL)	Growth medium (mL)	End volume (mL)
T25	5	2	6	10
T75	10	5	10	15
T175	15	7	13	30

COLLECTION OF PELLETS. HepG2- and Hepa1-6 cells were collected at passage 5 and 4-5, respectively. To collect adherent cells, the cell suspensions were centrifuged at 300xg. The supernatant was removed, 15 mL PBS was added to the tubes and the pellets were resuspended. Those re-suspended cells were centrifugated again at 300x*g* for 5 minutes, resulting in the formation of pellets. The supernatant was removed, and the pellets were stored at -20°C until needed for lysis.

For HepG2 cells, frozen pellets were also used. One of those pellets was stored at -80°C for a long period of time.

LYSATES FROM THE HEPA1-6 CELLS AND THE HEPG2 CELLS WERE PREPARED. To each tube, cold lysis buffer was added. How much buffer needed, depends on the size of the pellets. For small pellets (± 1 x 10^6 cells) 5 mL buffer was used, while 10 mL buffer was used for the larger pellets (± 5 x 10^7 cells). The cells were then vortexed every 5 minutes during half an hour. Throughout the process it is important to keep the tubes on ice to prevent protein degradation.

Next, the suspension was divided over microcentrifuge tubes, each containing 1 mL. These were then centrifuged at 14000x*g* for 15 minutes and the supernatant of each microcentrifuge tube was then transferred to a new set of microcentrifuge tubes. Those new tubes now contain the lysates of the Hepa1-6 and HepG2 cells and were stored in the freezer at a temperature of -20°C.

4.2.2 Detection of importin-α proteins in the soluble fractions of Hepa1-6 and HepG2 cells

One aliquot of each lysate (HepG2 and Hepa1-6) was thawed in hand and put on ice. Lysates were concentrated with 10K concentrator and samples of unconcentrated (1X), 2X, 5X and 10X concentrated lysates were prepared by mixing 30 µL sample with 10 µL 4x sample buffer and boiling them for 10 min. SDS-PAGE and a wet transfer were performed as described in section 4.2.6.

The primary monoclonal mouse anti-importin-α Ab (details in material section) was diluted 1/2000 in blocking buffer and incubated with the membrane for 2 h at room temperature (RT). Moreover, a secondary antibody (goat anti-mouse) conjugated with HRP was also used for detection. The WB was developed with the SuperSignal West Femto Maximum Sensitivity Substrate.

4.2.3 Protein Production

TRANSFORMATION. The plasmid pET21b-*Pbe*CSP$_{FL}$ was transformed into *E. coli* SHuffle® T7 Express cells for the recombinant production of *Pbe*CSP$_{FL}$. To produce *Pfa*CSP$_{FL}$, an existing glycerol stock of the same bacterial cell-line transformed with the pET21b-*Pfa*CSP$_{FL}$ plasmid was used.

An aliquot of 50 µL chemocompetent *E. coli* SHuffle® T7 Express cells was thawed on ice for 10 min. Subsequently, 50 ng of the pET21b-*Pbe*CSP$_{FL}$ expression vector was added to the cells and the suspension was incubated on ice for 30 min. Then a heat shock was applied by incubating the cell suspension for 45 s at 42°C in a water bath, after which the cells were incubated for 5 min on ice. The cells were then incubated with 950 µL SOC medium for 60 min at 37°C with agitation for recovery. Transformants were selected by plating 100 µL of undiluted and 10-fold diluted cell suspension (in SOC medium) on LB-agar plates supplemented with 100 µg/mL ampicillin and 2% glucose and overnight (ON) (upside-down) incubation at 37°C. The remaining undiluted cell suspension was spun down for 2 min at 14000 rpm. The cell pellet was re-suspended in 100 µL SOC medium and plated out as well.

PRE-CULTURES. Pre-cultures were started by inoculation of 10-15 mL 2xTY medium (supplemented with 100 µg/mL ampicillin and 0.2% glucose) with a single colony from the fresh transformation or some cell paste from an existing glycerol stock and ON incubation at 37°C with agitation.

PRODUCTION. Main cultures of 1x 1 L *Pbe*CSP$_{FL}$ and 3x 1 L for *Pfa*CSP$_{FL}$ 2xTY medium (supplemented with 100 µg/mL ampicillin and 0.2% glucose) were inoculated by the addition of 250-fold dilutions of pre-culture and incubated at 37°C with agitation. When the cell-cultures reached an $OD_{600\ nm}$ of 0.6 - 0.8, protein production was induced by the addition of isopropyl *β*-D-1-

thiogalactopyranoside (IPTG) to a final concentration of 1 mM and further incubated ON at 20°C with agitation.

PRODUCTION ANALYSIS. Culture samples of 1 mL were collected at different timepoints for SDS-PAGE and WB analysis: before induction (BI), 2 h after induction, 4 h after induction and after ON incubation. Samples were normalized against the BI sample. The appropriate volumes were centrifuged for 2 min at 14000 rpm, after which the cell pellets were re-suspended in 40 µL Milli-Q water and boiled for 10 min. After the samples were cooled down, 5 µL DNase I (with a stock concentration of 50 µg/mL) was added and incubated for 1 min. For SDS-PAGE analysis 4x sample buffer was added, and the samples were boiled for 10 mins.

CELL HARVESTING. The main cultures were centrifuged (Eppendorf Centrifuge 5810R, A-4-81 rotor) for 30 min at speed of 4000 rpm and 4°C. Each pellet from a 1 L culture was re-suspended in 40 mL lysis buffer A1, flash frozen in liquid nitrogen and stored at -20°C.

4.2.4 The purification of *Pfa*CSP$_{FL}$ and *Pbe*CSP$_{FL}$

Prior to purifying CSP, the *E. coli* cells were lysed by sonication. The target proteins in the soluble fractions were purified by chromatographic methods on the Akta Pure or Explorer purification platforms.

LYSIS. Aliquots of the cell suspensions were thawed at RT and 1:1 diluted with lysis buffer A1. Four different lysis methods were tested to lyse the cells containing *Pfa*CSP$_{FL}$, while for *Pbe*CSP$_{FL}$ only methods 1 and 2 were tested (Table 4.2).

Table 4.2 **DIFFERENT METHODS TO LYSE THE CELLS**

Method	Lysozyme (µg/mL)	Sonication
1	0	10 cycles (± 7 min): 10 s pulses, 20% amplitude, 30 s breaks
2	300	10 cycles (± 7 min): 10 s pulses, 20% amplitude, 30 s breaks
3	0	180 cycles (± 30 min): 5 s pulses, 20% amplitude, 5 s breaks
4	300	180 cycles (± 30 min): 5 s pulses, 20% amplitude, 5 s breaks

After sonication, the suspensions were transferred to 50 mL conical tubes and centrifuged for 30 minutes at 18000xg and 4°C to separate the soluble and insoluble fractions. Subsequently, the supernatant was filtered through a syringe filter (0.22 µm) to remove residual cellular debris.

Samples of the soluble and insoluble fractions were prepared for western blot (WB) analysis. The insoluble fractions were prepared by scraping off some pellet and re-suspending it in 0.5 mL MQ (for *Pfa*CSP$_{FL}$) or re-suspending the pellet in MQ to the initial volume prior to taking a 50 µL sample (for *Pbe*CSP$_{FL}$). In all cases (soluble and insoluble fractions), 50 µL samples were mixed with 20 µL 4x sample buffer and boiled for 10 min.

IMMOBILIZED METAL AFFINITY CHROMATOGRAPHY (IMAC). The first step is IMAC. A 5 mL HisTRAP HP was equilibrated with 5 column volumes (CVs) wash buffer (buffer A1), after which the sample was applied to the column at 2 mL/min (*Pfa*CSP$_{FL}$) or 1 mL/min (*Pbe*CSP$_{FL}$) with a peristaltic pump at 4°C. Prior to elution, the column was washed with 10 CVs wash buffer at 1 mL/min. The target protein was eluted via a gradient elution from 0 to 50% elution buffer (buffer B) over 20 CVs, followed by a step elution to 100% for 2 CVs, both at 1 mL/min.

Samples of the flow-through, wash fraction and specific elution fractions (based on chromatogram profile) were prepared by mixing 30 µL sample with 10 µL 4x sample buffer and boiling for 10 min. Per well 15 µL sample was loaded, after which SDS-PAGE and WB were executed as described in section 4.2.6.

SIZE EXCLUSION CHROMATOGRAPHY (SEC). A HiLoad 16/60 Superdex200 pg column was equilibrated with 2 CVs buffer C prior to injecting the relevant IMAC elution fractions. An isocratic elution over 1 CV was used to remove the remaining contaminants based on their molecular size. Relevant elution fractions were again subjected to SDS-PAGE analysis, as described in section 4.2.6.

HEPARIN AFFINITY CHROMATOGRAPHY (HAC). This last purification step had two purposes: i) it is used as a polishing step to remove the last remaining contaminants, and ii) it selects for functional and therefore biological relevant protein since heparin is a structural analog of HS-HSPGs. A 1 mL HiTRAP HP column was equilibrated with 5 CVs wash buffer (buffer C) prior to loading the relevant SEC fractions with a peristaltic pump at 0.2 mL/min and 4°C. Subsequently, the column was washed with 5 CVs wash buffer, after which the target protein was eluted via a gradient elution from 0 to 100% elution buffer (buffer D) over 40 CVs. Relevant HAC fractions were again analyzed by SDS-PAGE and WB, as described in section 4.2.6. Fractions containing the target protein were pooled and their concentration was determined by UV spectrophotometry. Aliquots of 250 µL were made and stored at 4°C or -20°C (after flash freezing in liquid nitrogen) until further use.

4.2.5 Pull-down assays

Multiple pull-downs were performed with *Pfa*CSP$_{FL}$ and *Pbe*CSP$_{FL}$ (as baits), and HepG2 and Hepa1-6 (as sources of importin-α proteins), using the QuickPick IMAC kit. Reaction mixtures of 0.5 mL were prepared by adding 25 µg CSP to 2X concentrated cell lysate and interaction was allowed for 2 h at room temperature. Two negative controls were incorporated by adding i) no CSP or ii) a non-relevant Nanobody instead of CSP, to the lysates. For each reaction, 100 µL magnetic beads was transferred to a microcentrifuge tube and activated by incubation in 400 µL regeneration buffer for 10 minutes. Subsequently, the beads were equilibrated in 400 µL wash buffer 1 and added to the reaction mixture. Capture of the his-tagged CSP by the beads was allowed for 30 minutes, after which the beads were washed in 400 µL wash buffer 2 for 2 minutes. Finally, proteins were eluted from the beads by incubation in 30 µL elution buffer for 10 minutes. The beads were discarded and all assay samples (reaction mixture or flow-through, wash fractions and elution fraction) were prepared for SDS-PAGE and WB by adding the appropriate amount of 4x sample buffer and boiling them for 10 min.

4.2.6 SDS-PAGE and Western blot

SDS-PAGE. For SDS-PAGE, 5 µL Precision plus protein dual color standard was loaded on 7.5% or 10% polyacrylamide gels as reference. Gels were run in 1x MES buffer for 40 - 60 min at 120 V. Protein bands were visualized by Coomassie Brilliant Blue R-250 (CBB R-250) or CBB G-250 staining. Background staining was removed with destaining solution or MQ, respectively.

WESTERN BLOT (WB). For WB, 7.5 µL protein marker was loaded on gel as reference. Proteins were transferred to a 0.45 µm nitrocellulose membrane (Bio-Rad) via a wet transfer in transform buffer for 1 h at 100 V and 250 mA. Residual binding sites were blocked ON in blocking buffer at 4°C while shaking. Between every solution change, the membrane was washed three times with PBST. The primary and secondary antibodies were mouse anti-His or mouse anti-importin-α and goat anti-mouse (conjugated with HRP), resp. The Abs were 2000-fold (anti-importin-α) or 4000 to 5000-fold (anti-His and anti-mouse) diluted in blocking buffer and incubated with the membrane for 1-2 h at room temperature. Prior to development, the membrane was washed once more with PBS. Development was performed with the Pierce CN/DAB Substrate Kit (anti-His WB) or SuperSignal West Femto Maximum Sensitivity Substrate (anti-importin-α WB).

CHAPTER V

RESULTS AND DISCUSSION

5.1 CELL CULTIVATION

The Hepa1-6 cells grew well and fast. In contrast, the HepG2 cells displayed some problems with bacterial contamination and there was also a risk of *Mycoplasma* contamination, as observed in the past. However, it is remarkable that only the HepG2 cells had issues with *Mycoplasma* contamination, while Hepa1-6 cells did not. It is possible that the contamination originates from the supplier of those HepG2 cells. Given the fact that other cell cultures were not contaminated, it means that all the work, after handling the HepG2 cells, was done aseptically. Another possibility is that the HepG2 cells may be more susceptible to *Mycoplasma* (60). Nonetheless, for researching the interaction between importin proteins and CSP, *Mycoplasma* contamination would not be as big of an issue regarding the outcome. On top of that, Mycoplasma contamination was solved by disinfecting the laboratories and attaining a new cell line.

5.2 IMPORTIN-α PROTEINS CAN BE DETECTED IN HEPATOCYTE LYSATES

One of the key factors of this research is to detect importin-α proteins in human and murine hepatocyte lysates. A commercial monoclonal anti-importin-α antibody was assessed in its ability to detect members of the importin-α protein family in hepatocyte cell lysates via a western blot (WB) assay. Different concentrations of lysates were tested to determine optimal detection conditions for the planned pull-down experiments. Single protein bands with a molecular mass typical for importin-α proteins (53 to 60 kDa) are detected in both lysates at all concentrations (Figure 5.1). This demonstrates that the antibody can detect members of the importin-α protein family in both Hepa1-6 (murine-origin) and HepG2 (human-origin) cell lysates. The signals in the lysates concentrated 5-fold or more (indicated by 5X and 10X in Figure 5.1) are blurry, probably due to oversaturation. Since the most abundant and clear signals were measured for the 2X concentrated lysates, this concentration was used as starting point for the pull-down experiments.

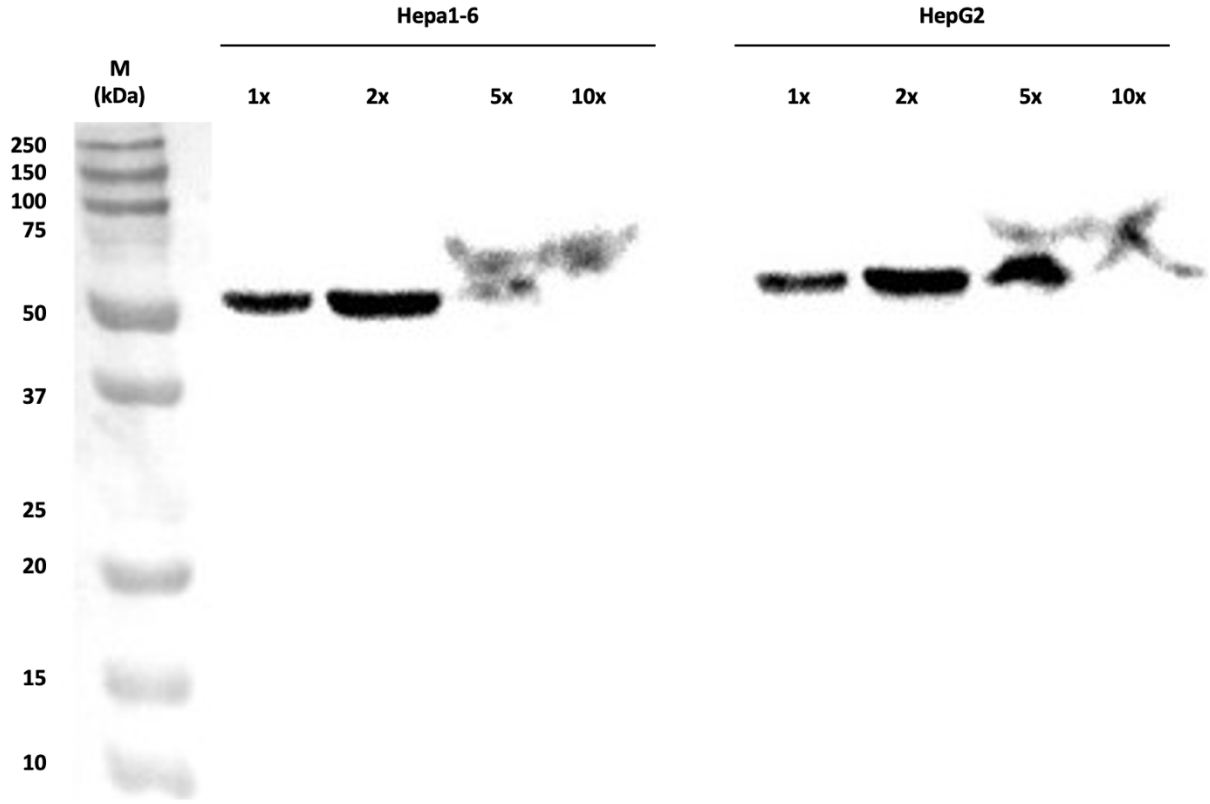

Figure 5.1 **IMPORTIN-α PROTEINS ARE DETECTED IN BOTH THE HEPA1-6 AND HEPG2 LYSATES.** Abbreviation: M = reference marker.

5.3 PROTEIN PRODUCTION

For the visualization of the progress of recombinant *Pfa*CSP$_{FL}$ and P*be*CSP$_{FL}$ production in *E. coli*, culture samples were collected at different time points and analyzed by SDS-PAGE and WB (Figure 5.2). This confirms the successful recombinant production of *Pfa*CSP$_{FL}$ and P*be*CSP$_{FL}$ in a bacterial system. The theoretical molecular masses (MM) of *Pfa*CSP$_{FL}$ and *Pbe*CSP$_{FL}$ based on their primary sequences are 40.996 kDa and 33.388 kDa, respectively. However, the proteins display higher electrophoretic mobilities which are consistent with observation made both in-house (R. Geens, unpublished results) and by other groups and may be explained by CSP's intrinsic disordered protein (IDP)-like properties (38, 61, 62) . As expected, no target proteins are observed in the samples before induction (BI), but only after inducing gene expression with IPTG from where the concentration increases over time.

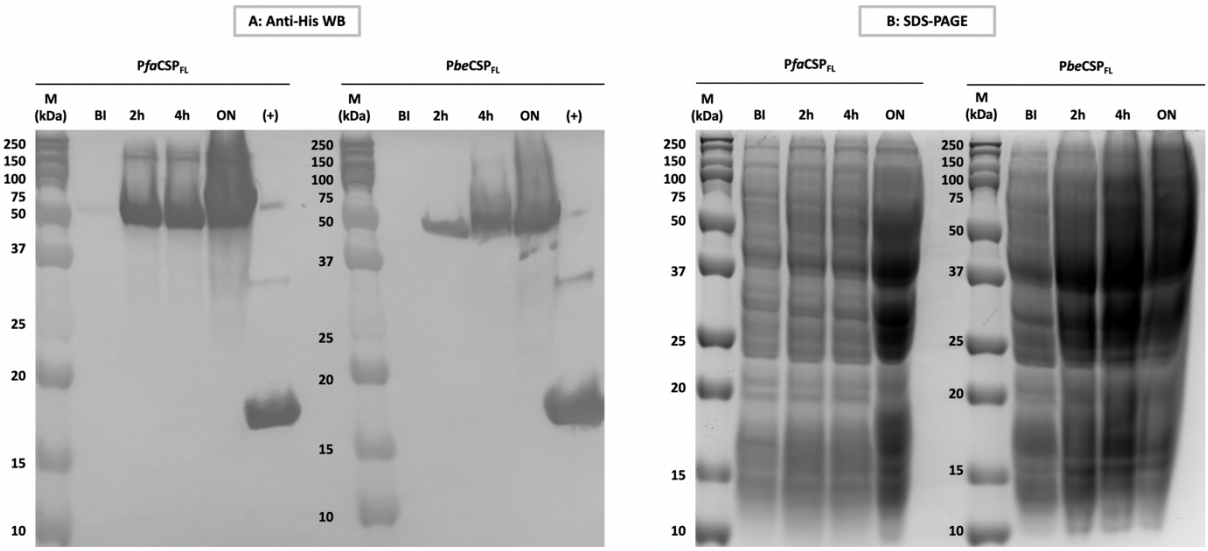

Figure 5.2 **RECOMBINANT PRODUCTION OF *Pfa*CSP$_{FL}$ AND *Pbe*CSP$_{FL}$**. Culture samples before-induction (BI), 2 h and 4 h post-induction (2h and 4h), and after overnight incubation (ON) were analyzed by (A) WB with an anti-His primary antibody and (B) SDS-PAGE (Coomassie Brilliant Blue (CBB)). 2.5 µg of a His-tagged Nanobody was used as positive control (+).

5.4 PROTEIN PURIFICATION

5.4.1 Cell lysis: the detection of *Pfa*CSP$_{FL}$ and *Pbe*CSP$_{FL}$ in the lysates

Several lysis conditions were tested to optimize cell lysis of *E. coli* containing the recombinantly produced target proteins in their cytoplasm. In the case of *Pfa*CSP$_{FL}$, four different lysis conditions were tested in which two sonication protocols were compared with and without pre-incubation with lysozyme. WB shows that all conditions result in soluble target protein, but none yields significantly higher amounts compared to the others (Figure 5.3A). For *Pbe*CSP$_{FL}$, only two lysis conditions were compared using the same sonication protocol with and without lysozyme. Here the amount of target protein present in the insoluble and soluble fractions was also compared by maintaining equal volumes. Although some target protein can be observed in the insoluble fractions, the major part is soluble (Figure 5.3B). No significant differences can be observed between the lysis conditions based on the WB analysis.

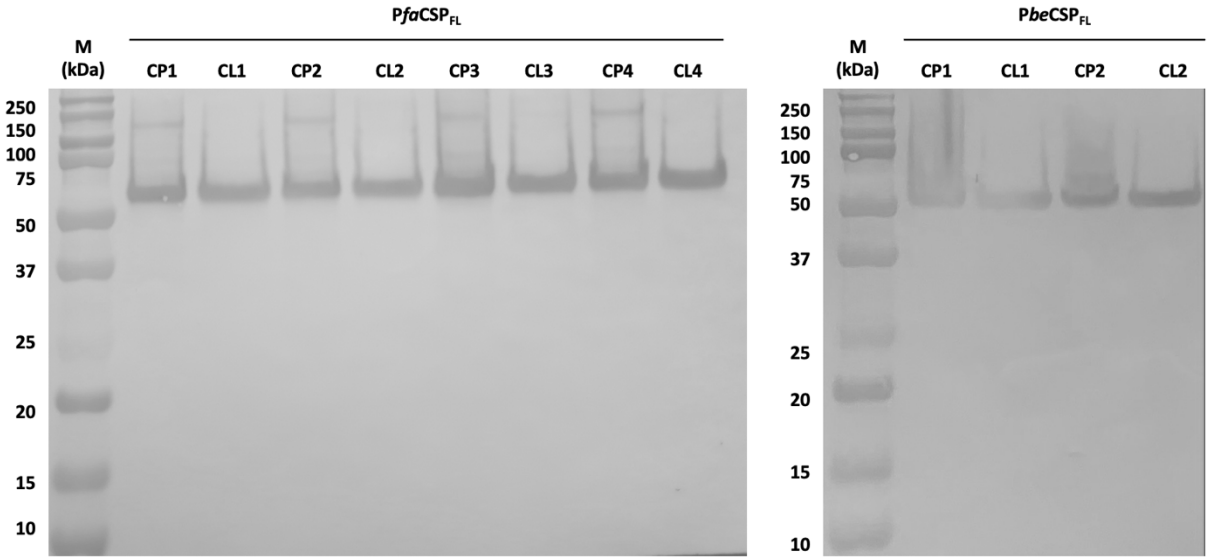

Figure 5.3 **COMPARISON OF CELL LYSIS CONDITIONS FOR *E. Coli* CONTAINING (A) *Pfa*CSP$_{FL}$ AND (B) *Pbe*CSP$_{FL}$ BY WESTERN BLOTTING.** Abbreviations: CP = cell pellet (insoluble fraction), CL = cell lysate (soluble fraction).

5.4.2 Purification of P*fa*CSP$_{FL}$

*Pfa*CSP$_{FL}$ is purified by a three-step protocol comprising immobilized metal affinity chromatography (IMAC) and size exclusion chromatography (SEC) to remove the bulk of contaminants, and heparin affinity chromatography (HAC) as a last polishing step. The HAC also serves a second function as it selects for functional (and thus biologically relevant) proteins since heparin is structural analogue of liver HS-HSPGs, CSP's natural binding partner.

As observed from the IMAC elution profile, two peaks emerge starting from 10% elution buffer. SDS-PAGE and WB analyses show that *Pfa*CSP$_{FL}$ is mainly present in fractions 4 to 15. These fractions correspond to the first peak of the elution profile (grey arrow in Figure 5.4A). The remaining contaminants were removed by SEC. The SEC chromatogram displays one large peak which eluted at approximately 65 mL and SDS-PAGE reveals that it mainly contains *Pfa*CSP$_{FL}$, together with some smaller impurities (Figure 5.4B). The last impurities were removed for the most part by the final purification step, HAC. The HAC elution profile of *Pfa*CSP$_{FL}$ typically displays a landscape of elution peaks as can also be observed in the chromatogram (Figure 5.4C). SDS-PAGE and WB analyses show that most *Pfa*CSP$_{FL}$ is biological relevant since it binds to heparin and eluted between 155 and 365 mM NaCl, which is consistent with previous reports in the literature (39). Some minor contaminants around 25 kDa are still present, however, the final purity of *Pfa*CSP$_{FL}$ is sufficient for the pull-down assays. The recombinant production and purification of *Pfa*CSP$_{FL}$ yielded 1.51 mg per liter of bacterial culture and aliquots at 0.5 mg/mL were prepared.

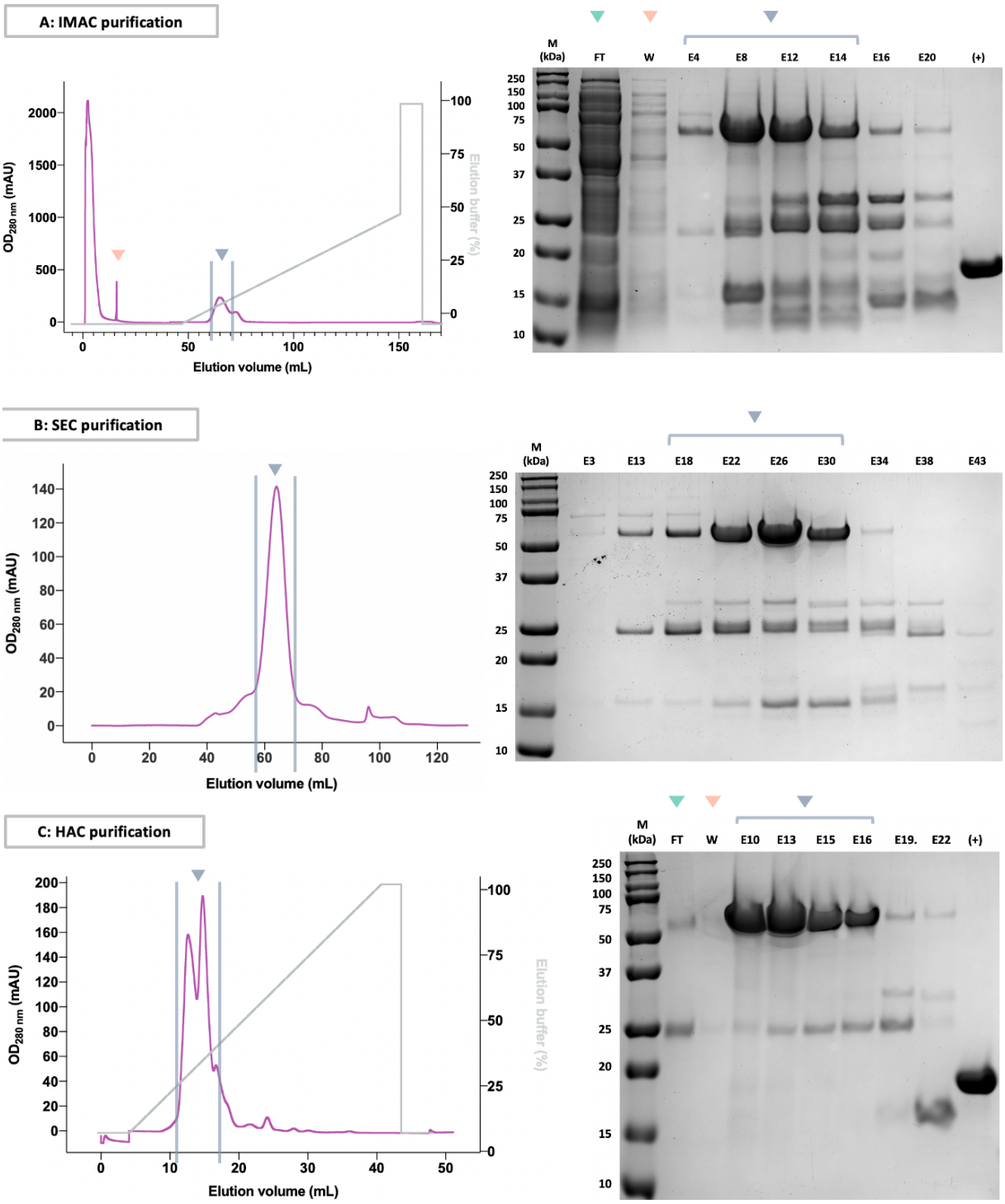

Figure 5.4 **PURIFICATION OF *Pfa*CSP$_{FL}$.** (A) IMAC purification: fractions were selected for analysis based on the chromatogram (purple curve) with elution buffer B (grey curve): flow-through (green arrow), wash (orange arrow), elution peak harboring most *Pfa*CSP$_{FL}$ (grey arrow). (B) SEC purification: fractions were chosen for analysis based on the elution profile (purple curve). (C) HAC purification: fractions were selected for analysis based on the elution profile (purple curve) with elution buffer D (grey curve): flow-through (green arrow), wash (orange arrow), elution fractions containing most *Pfa*CSP$_{FL}$ (grey arrow). The SDS-PAGEs were performed with CBB. Abbreviations: M = reference marker, FT = flow-through, W = wash, E = elution, (+) = positive control.

5.4.3 Purification of *Pbe*CSP$_{FL}$

*Pbe*CSP$_{FL}$ is purified through the same protocol as *Pfa*CSP$_{FL}$ and the results obtained are very similar. In the IMAC elution profile, a peak can be observed starting from 5% buffer. The target protein is mainly present in fractions 11 till 20. Those fractions correspond with the peak (grey arrow) in the elution profile (Figure 5.5A). The SEC chromatogram reveals different peaks, and the elution starts from approximately 50 mL (Figure 5.5B). Elution fractions 9 till 21 contain the most target protein, corresponding to the first two peaks (grey arrow) in the elution profile. The remaining and last contaminants were mostly removed by HAC. *Pbe*CSP$_{FL}$ is biologically relevant and eluted between 140 and 420 mM NaCl and the final purity of *Pbe*CSP$_{FL}$ is sufficient for the pull-down assays (Figure 5.5C). Finally, the recombinant production and purification of *Pbe*CSP$_{FL}$ yielded 2.15 mg per liter of bacterial culture and aliquots at 0.5 mg/mL were prepared.

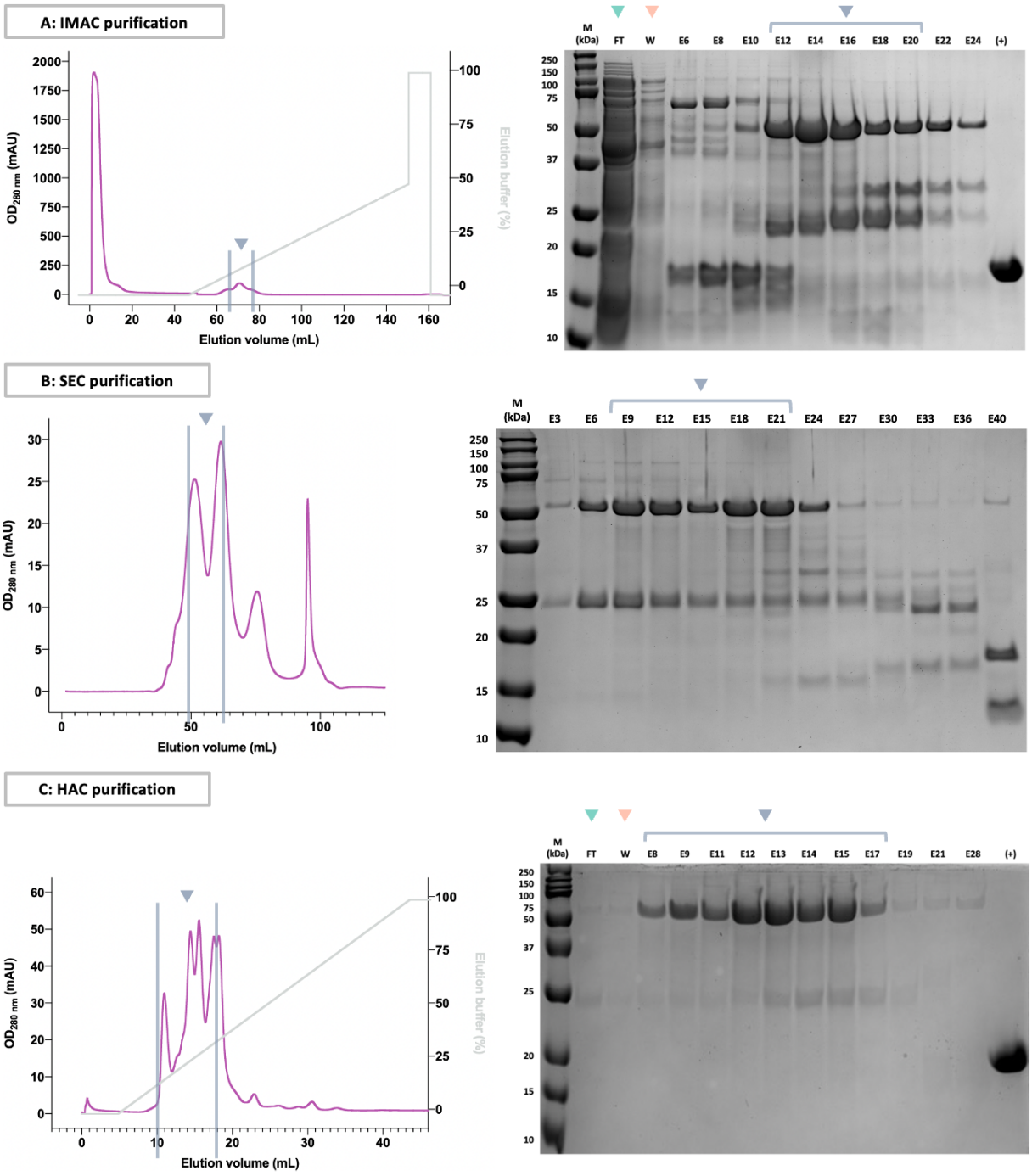

Figure 5.5 **PURIFICATION OF *Pbe*CSP$_{FL}$**. (A) IMAC purification: fractions were chosen for analysis based on the elution profile (purple curve), elution buffer A (grey curve), fractions that contained the most *Pbe*CSP$_{FL}$ (grey arrow), wash (orange arrow), flow-through (green arrow) (B) SEC purification: fractions were chosen for analysis based on the elution profile (purple curve), fractions that contained the most *Pbe*CSP$_{FL}$ (grey arrow). (C) HAC purification: fractions were chosen for analysis based on the elution profile (purple curve), elution buffer D (grey curve), fractions that contained the most *Pbe*CSP$_{FL}$ (grey arrow), wash (orange arrow), flow-through (green arrow). The SDS-PAGEs were performed with CBB. Abbreviations: M = reference marker FT = flow-through, W = wash, E = elution, (+) = positive control.

5.5 PERFORMING PULL-DOWN ASSAYS AS THE LAST STEP

For the detection of a possible interaction between the CSP and members of the importin-α protein family, several pull-down assays were performed. The lysates of two hepatocyte cell-lines were used as sources of importin-α proteins (*"prey"*): HepG2 (human-derived) and Hepa1-6 (murine-derived). Recombinant *Pfa*CSP$_{FL}$ and *Pbe*CSP$_{FL}$ (*"bait"*) were added to the hepatocyte lysates to investigate whether an interaction partner would bind (*"catching prey")*. Nickel-coated magnetic beads were subsequently used as affinity ligand to capture the hexahistidine-tagged CSPs. The various fractions obtained during the assay were analyzed by SDS-PAGE and WB. In the next sections, the optimization and results of the pull-downs will be discussed.

5.5.1 The first round of pull-down assays

During the first pull-down assays, the interactions between *Pfa*CSP$_{FL}$ and *Pbe*CSP$_{FL}$ with Hepa1-6 and HepG2 importin-α proteins were tested.

SDS-PAGE and anti-His WB show that both *Pfa*CSP$_{FL}$ and *Pbe*CSP$_{FL}$ are present in the elution, while little is left in the wash and flow-through (Figure 5.6A and Supplementary figure S1). This demonstrates that the experimental set-up is valid since the antigen capturing by and the subsequent elution from the affinity ligand was successful. The small amounts of CSP in the flow-through and wash fraction indicate that not all CSP could bind to the beads. This may be explained by the limited capture capacity of the beads and the relatively high amount of CSP used during the pull-downs. On top of that, the signals of the anti-His WB look cluttered because of oversaturation due to the combination of the high amount of CSP and the use of an extremely sensitive substrate.

Based on the anti-importin-α WB, only importin-α proteins from the Hepa1-6 lysates have possibly interacted with *Pfa*CSP$_{FL}$ and *Pbe*CSP$_{FL}$ (Figure 5.6B). However, the signals are rather weak, especially in the case of the pull-down with *Pbe*CSP$_{FL}$. It should be noted that these first pull-downs with *Pbe*CSP$_{FL}$ were performed with a mix of the two lysates due to a manual error. Furthermore, only the Hepa1-6 positive control shows a signal, in contrast to the HepG2 control (Figure 5.6B). This means that even if there is an interaction between those HepG2 importin-α proteins and the CSP, it cannot be detected. This is a strange outcome since importin-α proteins were detected in both the Hepa1-6 and HepG2 lysates and most human and mouse homologs display a high sequence identity (Figure 5.1 and Supplementary table S1).

A possible explanation might be that more sample should be loaded for anti-importin-α WB. Another possibility is that this problem may lie in the different batches, because there were originally two batches from both the Hepa1-6 and HepG2 lysates. This is especially the case for the HepG2 lysates, since one batch contained freshly cultivated cells, while the other contained frozen pellets. One of those frozen pellets was stored at -80°C for a long time, which may have an impact on the structural integrity of the importin-α proteins. To examine whether there is a difference between those batches, an additional WB was performed. However, the WB demonstrated that there are no significant differences in the detection of importin-α proteins between the batches (Supplementary figure S2).

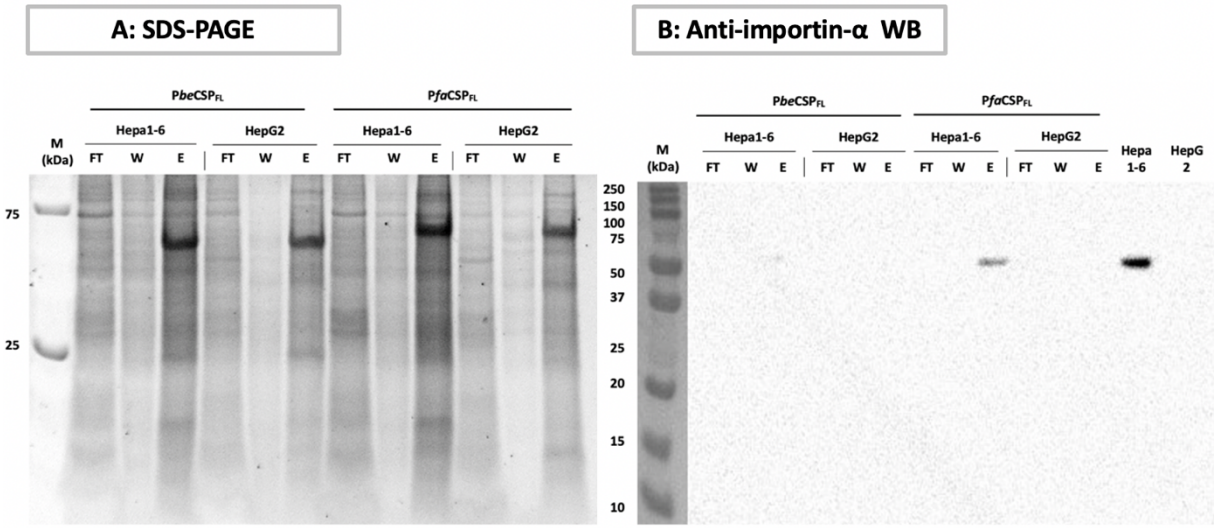

Figure 5.6 **FIRST ROUND OF PULL-DOWN ASSAYS**. (A) SDS-PAGE with oriole staining. (B) Anti-importin-α WB. Abbreviations: M = reference marker, FT = flow-through, W = wash, E = elution, (+) = positive control.

5.5.2 The second round of pull-down assays

To optimize the assay, 35 µL of the samples was loaded (instead of 15 µL) for analysis. Therefore, three pull-down assays were performed in parallel (one for each analysis: SDS-PAGE, anti-His WB and anti-importin-α WB). Moreover, to obtain stronger signals for the elution fractions in the anti-importin-α WB, 30 µL elution fraction with 10 µL sample buffer was used instead of 30 µL of both elution fraction and sample buffer. The HepG2 lysates were concentrated 5X (instead of 2X).

For the *Pbe*CSP$_{FL}$-Hepa1-6 pull down, there are clearly importin-α proteins present in the elution, but also in the flow-through and some were also left behind in the wash fraction, which may suggest that the *Pbe*CSP$_{FL}$ – importin-α interaction displays a low affinity (Figure 5.7A). With regards to the *Pbe*CSP$_{FL}$-HepG2 pull-down, the HepG2 positive control now shows a signal, which was not the case before (Figure 5.6B and Figure 5.7B). Some importin-α proteins were left behind in the flow-through,

while little reached the elution (Figure 5.7B). But once again the results for HepG2 are not clear enough even though the lysate was concentrated 5X and more sample was loaded for analysis. For the P*fa*CSP$_{FL}$-Hepa1-6 pull-down, the WB results show that there are importin-α proteins in the elution fraction. This may imply an interaction with the Hepa1-6 importin-α proteins and *Pfa*CSP$_{FL}$. But this was not the case with HepG2 importin-α proteins. The HepG2 positive control does not show a signal (Figure 5.7C). It should be noted that the pull-downs with *Pbe*CSP$_{FL}$ and *Pfa*CSP$_{FL}$ were executed separately as were the concentrations of the lysates.

The problem with the HepG2 importin-α proteins is still present. This resulted in the preparation of a third batch of HepG2 lysates. However, no importins were detected, hence the fresh HepG2 lysates could not be used for the pull-down assays. It was observed that HepG2 cells were more difficult to work with than Hepa1-6 cells. Only Hepa1-6 lysates were used during the next assays.

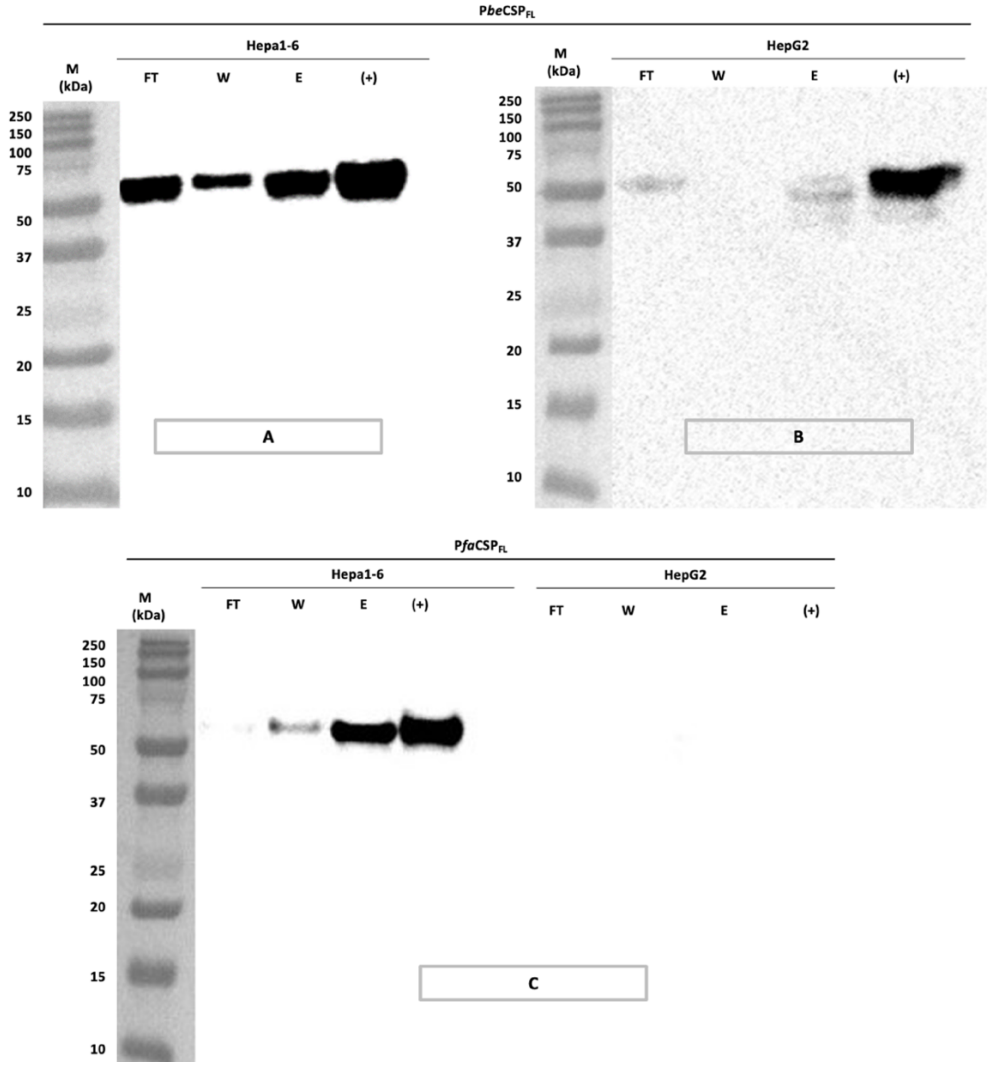

Figure 5.7 **SECOND ROUND OF PULL-DOWN ASSAYS: HEPA1-6 IMPORTIN-α PROTEINS SHOW AN INTERACTION WITH *Pbe*CSP$_{FL}$ AND *Pfa*CSP$_{FL}$.** Anti-importin-α WBs of (A) the *Pbe*CSP$_{FL}$-Hepa1-6 pull-down, (B) the *Pbe*CSP$_{FL}$-HepG2 pull down, and (C) the *Pfa*CSP$_{FL}$ pull-downs with Hepa1-6 and HepG2 lysates. Abbreviations: M = reference marker, FT = flow-through, W = wash, E = elution, (+) = positive control.

5.5.3 The third round of pull-down assays

This time, assays with only magnetic beads (MBs) and a non-relevant hexahistidine-tagged nanobody (Nb), instead of *Pfa*CSP_{FL} or *Pbe*CSP_{FL}, were included as negative controls. On top of that, 7.5% gels (instead of 10%) were used for the analysis of the pull-downs with *Pfa*CSP_{FL} and *Pbe*CSP_{FL}, such to increase the separation of proteins between 50 and 75 kDa. Moreover, an additional washing step (W2) was added to ensure that as little impurities as possible would be transferred to the elution.

It is expected to detect CSP and importin-α proteins in the elution fraction to conclude that there is an interaction. Indeed, for the *Pbe*CSP_{FL} as for the *Pfa*CSP_{FL} pull-downs, the importin-α proteins and CSP are both present in the elution fraction (Figure 5.8A-B and Supplementary figure S5). In case of the importin-α proteins, a considerable amount stayed behind in the flow-through as well. Altogether, these results are in agreement with those of the second round of pull-down assays and it may indicate that an interaction took place.

For the samples containing only magnetic beads and importin-α proteins, it is expected that only the anti-importin-α WB shows a signal in the flow-through sample. However, no signal is observed in any of the fractions (Figure 5.8C). This may indicate that importin-α proteins bind non-selectively to the beads, because the bounded importin-α proteins were discarded with the beads.

A non-relevant Nb was used as another control to make sure that the pull-down assays are valid. The Nb is not expected to interact with importin-α proteins, meaning that the importins should stay behind in the flow-through, while the Nb is transferred to the elution fraction. But the anti-importin-α WB shows no signal, not even in the flow-through (Figure 5.8F). In the elution fraction on the anti-His WB and the SDS-PAGE, Nbs can indeed be detected (Figure 5.8G-H). This once again possibly shows that the hypothesis of non-selective binding may be true. However, to test whether this hypothesis of non-selective binding is true, another round of pull-down assay could be performed in the future.

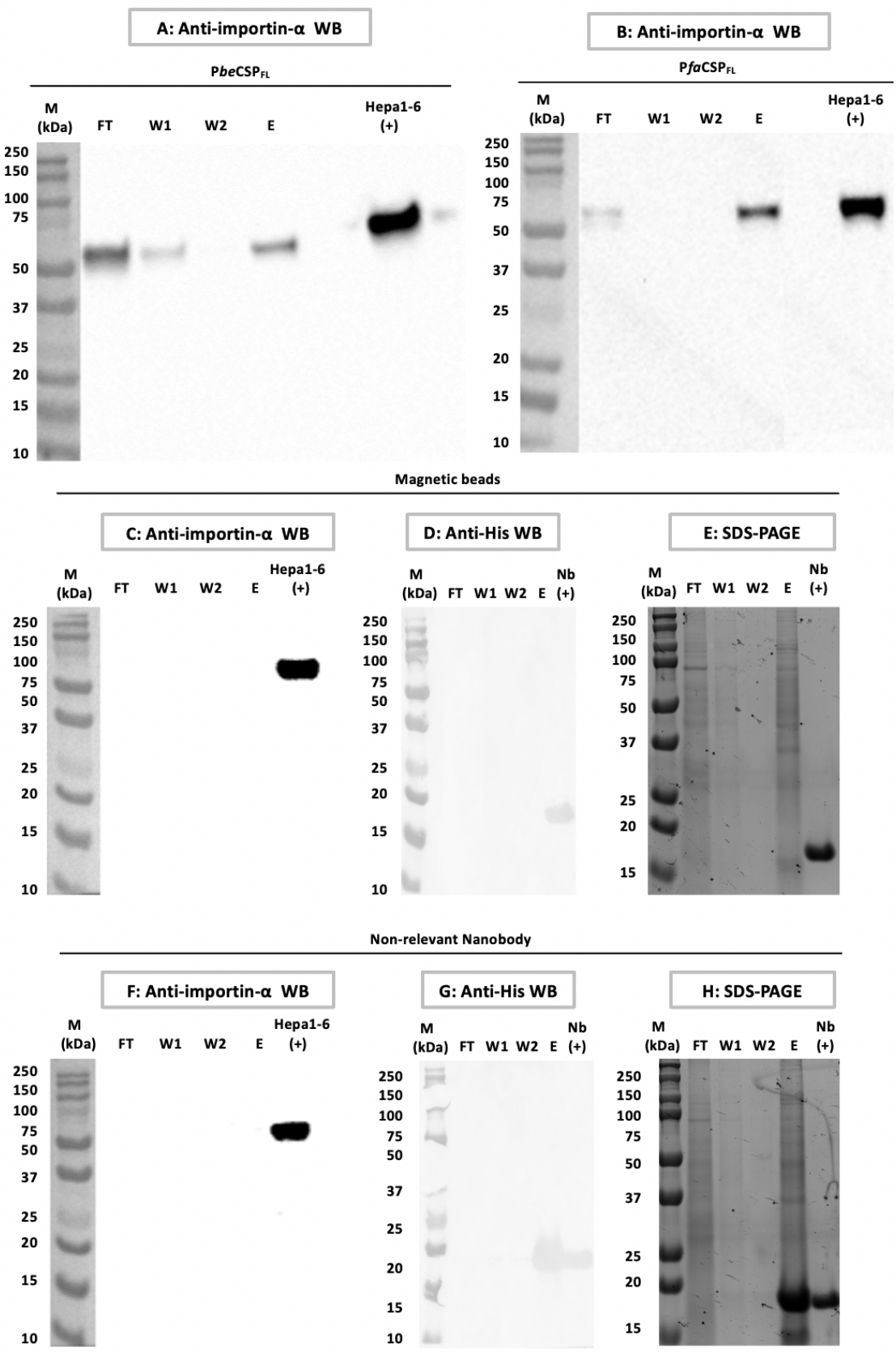

Figure 5.8 **THIRD ROUND OF PULL-DOWN ASSAYS: HEPA1-6 IMPORTIN-α PROTEINS SHOW AN INTERACTION WITH *Pbe*CSP$_{FL}$.** (A) Anti-importin-α WB (*Pbe*CSP$_{FL}$). (B) Anti-importin-α WB (*Pfa*CSP$_{FL}$). (C-E) Magnetic beads as sample: (C) anti-importin-α WB, (D) anti-His WB, and (E) SDS-PAGE (CBB). (F-H) Nanobodies as sample: (F) anti-importin-α WB, (G) anti-His WB, and (H) SDS-PAGE (CBB staining). Abbreviations: MB = magnetic bead, Nb = nanobody, M = protein marker, FT = flow-through, W = wash, E = elution, (+) = positive control.

CHAPTER VI

CONCLUSION

During this thesis, an attempt was made to validate the interaction between *Pbe*CSP$_{FL}$ and members of the importin-α protein family and to investigate whether a similar interaction exists for *Pfa*CSP$_{FL}$. *Pbe*CSP$_{FL}$ and *Pfa*CSP$_{FL}$ were successfully recombinantly produced in *E. coli* SHuffle® T7 Express and purified by various chromatographic techniques. Hepa1-6 (murine hepatocyte cell-line) and HepG2 (human hepatocyte cell-line) cells were cultivated, and lysates were prepared to serve as sources of importin-α proteins.

Importin-α proteins were detected in the cultivated hepatocyte lysates at different concentrations through WB with a monoclonal anti-importin-α primary antibody. The clearest signal was observed in lysates that were concentrated two times for both cell types. This was used as starting point for the pull-downs.

The obtained results indicate a possible interaction of both *Pfa*CSP$_{FL}$ and *Pbe*CSP$_{FL}$ with murine importin-α proteins. However, it cannot be excluded that the importin-α proteins interact non-specifically with the beads. For the HepG2 importin proteins, the results are not clear but based on the second round of pull-downs there is a possible interaction with *Pbe*CSP$_{FL}$. *Pfa*CSP$_{FL}$ was not observed to interact with HepG2 importins. But, because there were not that many pull-downs performed with HepG2 lysates (due to some issues with the lysates), the conclusion is incomplete. To have a better view, more pull-down assay with HepG2 still must be performed. Since it was observed that HepG2 cells could be problematic, the cultivation and processing of the lysates should be optimized.

Despite performing third rounds of pull-downs and optimizing every round, no unambiguous evidence of the interaction between importin-α proteins and CSP could be formed and further investigation is required to unequivocally demonstrate an interaction (or non-interaction).

CHAPTER VII

ANDERSTALIGE SAMENVATTING

Malaria is één van de vier dodelijkste infectieziekten en wordt overgebracht door de vrouwelijke *Anopheles* mug. Deze aandoening wordt veroorzaakt door parasieten van het *Plasmodium* genus. De levenscyclus begint met de aanwezigheid van sporozoïeten (SPZn) in de bloedbaan van de menselijke gastheer als gevolg van een beet van een geïnfecteerde mug. Deze SPZn kunnen vervolgens de levercellen bereiken en deze binnendringen met behulp van de interactie tussen hun belangrijkste oppervlakte-eiwit, het circumsporozoïet proteïne (CSP), en hoog-gesulfateerde heparaansulfaatgroepen op de levercellen. Eenmaal in de levercel, wordt verondersteld dat CSP in het cytoplasma terechtkomt en het transport van de transcriptiefactoren naar de celkern verhindert. Op deze manier zou het immuunsysteem van de levercel mogelijk onderdrukt worden en de overleving van de parasiet bevorderd worden. Pas wanneer de parasiet de bloedfase bereikt, is er sprake van ziekteverschijnselen zoals de kenmerkende koortsaanvallen. Het is van belang dat malaria goed en op tijd wordt behandeld om verdere complicaties te voorkomen. Als behandeling kan er gebruik gemaakt worden van chloroquine- en artemisine-gebaseerde therapieën. De stijgende resistentie tegen deze behandelingen is echter een stimulans voor het vinden van nieuwe middelen.

Het doel van deze thesis was om te onderzoeken of er een interactie plaatsvindt tussen de importine-α eiwitten en het CSP van zowel *P. falciparum* als *P. berghei.* Om dit te bereiken werden *Pfa*CSP_{FL} en *Pbe*CSP_{FL} recombinant geproduceerd in *E. coli* en opgezuiverd via chromatografische methoden. Voor het verkrijgen van de importine-α eiwitten van zowel menselijke als murine oorsprong, werden respectievelijk HepG2 en Hepa1-6 cellen gecultiveerd. Tenslotte werden pull-down assays uitgevoerd om de mogelijke interactie tussen CSP en importine-α eiwitten te onderzoeken

CHAPTER VIII

PERSPECTIVES

Although the pull-downs hint at a possible interaction between importin-α proteins and CSP, we were unable to provide unambiguous evidence to support the hypothesis. More clarity can be gained by further optimizing the pull-down assays or using other protein detection analyses. Because there were a lot of problems with HepG2 cells, it may also be interesting to recombinantly produce the importin-α proteins instead of cultivating liver cells. Since it seems that the CSP-importin-α interaction may display a low affinity, a label transfer interaction analysis could be a better option (63).

To further optimize the pull-down assays, it can be interesting to differentiate the importin-α proteins into importin-α1, 3, 4, 5, 6 and 7. This way, interaction can be measured with the different importin-α proteins.

On top of this, performing further pull-down assays may give out some clearness about the theory of possible non-selective binding of importin-α proteins with the magnetic beads (MBs). To realize this, a buffer that breaks the interaction between the MBs and the nickel (*"stripping"*) can be added. If importin-α proteins are bound non-selectively to the MBs, then it is expected to detect a signal in the stripping fraction.

CHAPTER IX

SUMMARY

Malaria is one of the 'Big Four' deadliest human-infectious disease and is transmitted by the female *Anopheles* mosquito. This disease is caused by parasites from the *Plasmodium* genus. The lifecycle starts with the presence of sporozoites (SPZn) in the bloodstream of the human host as a result of a bite from an infected mosquito. These SPZn can then reach and enter the liver cells through the interaction between one of their major surface proteins, the circumsporozoite protein (CSP), and the highly sulfated heparan sulfate proteoglycans on the liver cells. It is speculated that, once inside the liver cell, CSP can enter the cytoplasm and possibly prevent the transport of some transcription factors to the nucleus of the liver cell. This may result in the dampening of the inflammatory responses and thus promote the survival of the parasite. Once the parasite reaches the blood phase, symptoms such as the characteristic fever attacks can occur. It is important that malaria is treated properly and on time to prevent further complications. Chloroquine- and artemisin-based therapies can be used as treatment. However, the increasing resistance against these treatments is a motive to find new ways to combat or treat malaria.

The aim of this thesis was to investigate whether there is an interaction between the importin-α proteins and the CSP of both *P. falciparum* and *P. berghei*. To achieve this, *Pfa*CSP_{FL} and *Pbe*CSP_{FL} were recombinantly produced using *E. coli* cells and purified using chromatographic techniques. To obtain both human and murine importin-α proteins, respectively HepG2 and Hepa1-6 cells were cultivated. Finally, pull-down assays were performed to investigate whether there is a possible interaction between CSP and importin-α proteins.

LIST OF REFERENCES

1. Chen D-S, Locarnini S, Wallace J. From the big three to the big four. The Lancet Infectious Diseases. 2015;15(6):626-7.
2. Treating malaria: World Health Organization; 2020 [cited 2020 6 dec.]. Available from: https://www.who.int/activities/treating-malaria.
3. Global Health DoPDaM. Malaria: Disease: Centers for Disease Control and Prevention; [updated January 4, 2019. Available from: https://www.cdc.gov/parasites/malaria/index.html.
4. Ploemen IHJ. Development and Demise of *Plasmodium* Liver Stage Parasites: Radboud Universiteit Nijmegen; 2013.
5. Singh AP, Buscaglia CA, Wang Q, Levay A, Nussenzweig DR, Walker JR, et al. *Plasmodium* Circumsporozoite Protein Promotes the Development of the Liver Stages of the Parasite. Cell. 2007;131(3):492-504.
6. Duffy PE, Patrick Gorres J. Malaria vaccines since 2000: progress, priorities, products. npj Vaccines. 2020;5(1):48.
7. Piperaki ET, Daikos GL. Malaria in Europe: emerging threat or minor nuisance? Clinical microbiology and infection : the official publication of the European Society of Clinical Microbiology and Infectious Diseases. 2016;22(6):487-93.
8. Roy LD. Meisje sterft aan malaria in Italië vrt nws: vrt nws; 2017 [Available from: https://www.vrt.be/vrtnws/nl/2017/09/05/meisje-sterft-aan-malaria-in-italie/.
9. Schepens W. Onderzoek bevestigt: koppel uit Kampenhout stierf aan malaria na steek van meegereisde mug vrt nws: Belga; 2020 [Available from: https://www.vrt.be/vrtnws/nl/2020/11/04/onderzoek-van-itg-bevestigt-koppel-uit-kampenhout-stierf-aan-ma/#:~:text=Control%20and%20Prevention-,Onderzoek%20bevestigt%3A%20koppel%20uit%20Kampenhout%20stierf%20aan%20malaria%20na%20steek,Die%20hebben%20ze%20niet%20gevonden.
10. Beck T. Will malaria soon be a thing of the past? the potential of recombinant protein vaccines to control one of the world's most deadly diseases. 2016 june 26. In: Dean L, McEntyre J, editors Coffee Break: Tutorials for NCBI Tools [Internet].
: Bethesda (MD): National Center for Biotechnology Information (US); 1999-; [Figure 1, [The malaria parasite life cycle...]]. Available from: https://www.ncbi.nlm.nih.gov/books/NBK5951/figure/malaria_LifeCycle/.
11. Miller LH, Ackerman HC, Su XZ, Wellems TE. Malaria biology and disease pathogenesis: insights for new treatments. Nature medicine. 2013;19(2):156-67.
12. Cowman AF, Healer J, Marapana D, Marsh K. Malaria: Biology and Disease. Cell. 2016;167(3):610-24.
13. the editors of Salem P. Magill's medical guide : health and illness: Pasadena, Calif. : Salem Press, c1995-c1996.; 1995.
14. Gazzinelli RT, Kalantari P, Fitzgerald KA, Golenbock DT. Innate sensing of malaria parasites. Nature reviews Immunology. 2014;14(11):744-57.
15. Bhatt S, Weiss DJ, Cameron E, Bisanzio D, Mappin B, Dalrymple U, et al. The effect of malaria control on *Plasmodium falciparum* in Africa between 2000 and 2015. Nature. 2015;526(7572):207-11.
16. Pryce J, Richardson M, Lengeler C. Insecticide-treated nets for preventing malaria. The Cochrane database of systematic reviews. 2018;11(11):Cd000363.
17. Protopopoff N, Wright A, West PA, Tigererwa R, Mosha FW, Kisinza W, et al. Combination of Insecticide Treated Nets and Indoor Residual Spraying in Northern Tanzania Provides Additional Reduction in Vector Population Density and Malaria Transmission Rates Compared to Insecticide Treated Nets Alone: A Randomised Control Trial. PloS one. 2015;10(11):e0142671.

18. Paton DG, Childs LM, Itoe MA, Holmdahl IE, Buckee CO, Catteruccia F. Exposing Anopheles mosquitoes to antimalarials blocks *Plasmodium* parasite transmission. Nature. 2019;567(7747):239-43.
19. Paton DG, Probst AS, Ma E, Adams KL, Shaw WR, Singh N, et al. Antimalarials in mosquitoes overcome *Anopheles* and *Plasmodium* resistance to malaria control strategies. bioRxiv. 2021:2021.03.12.435188.
20. Loomans L, Conesa Botella A, D'Hondt A, Verschueren J, Van den Bossche D, Van Esbroeck M, et al. Accuracy of malaria diagnosis by clinical laboratories in Belgium. Malar J. 2019;18(1):104-.
21. White NJ, Pukrittayakamee S, Hien TT, Faiz MA, Mokuolu OA, Dondorp AM. Malaria. The Lancet. 2014;383(9918):723-35.
22. van der Pluijm RW, Amaratunga C, Dhorda M, Dondorp AM. Triple Artemisinin-Based Combination Therapies for Malaria – A New Paradigm? Trends in Parasitology. 2021;37(1):15-24.
23. Uwimana A, Umulisa N, Venkatesan M, Svigel SS, Zhou Z, Munyaneza T, et al. Association of *Plasmodium falciparum* kelch13 R561H genotypes with delayed parasite clearance in Rwanda: an open-label, single-arm, multicentre, therapeutic efficacy study. The Lancet Infectious diseases. 2021.
24. Coelho C, Doritchamou J, Zaidi I, Duffy P. Advances in Malaria Vaccine Development: Report from the 2017 Malaria Vaccine Symposium. npj Vaccines. 2017;2.
25. Draper S, Sack B, King C, Nielsen C, Rayner J, Higgins M, et al. Malaria Vaccines: Recent Advances and New Horizons. Cell Host and Microbe. 2018;24:43-56.
26. Zenklusen I, Jongo S, Abdulla S, Ramadhani K, Lee Sim BK, Cardamone H, et al. Immunization of Malaria-Preexposed Volunteers With *Pf*SPZ Vaccine Elicits Long-Lived IgM Invasion-Inhibitory and Complement-Fixing Antibodies. The Journal of infectious diseases. 2018;217(10):1569-78.
27. Ishizuka AS, Lyke KE, DeZure A, Berry AA, Richie TL, Mendoza FH, et al. Protection against malaria at 1 year and immune correlates following PfSPZ vaccination. Nature medicine. 2016;22(6):614-23.
28. Mordmüller B, Surat G, Lagler H, Chakravarty S, Ishizuka AS, Lalremruata A, et al. Sterile protection against human malaria by chemoattenuated PfSPZ vaccine. Nature. 2017;542(7642):445-9.
29. Sinnis P, Coppi A. A long and winding road: the *Plasmodium* sporozoite's journey in the mammalian host. Parasitology international. 2007;56(3):171-8.
30. De Niz M, Burda PC, Kaiser G, Del Portillo HA, Spielmann T, Frischknecht F, et al. Progress in imaging methods: insights gained into *Plasmodium* biology. Nature reviews Microbiology. 2017;15(1):37-54.
31. Dundas K, Shears MJ, Sun Y, Hopp CS, Crosnier C, Metcalf T, et al. Alpha-v–containing integrins are host receptors for the *Plasmodium falciparum* sporozoite surface protein, TRAP. Proceedings of the National Academy of Sciences. 2018;115(17):4477.
32. Kori LD, Valecha N, Anvikar AR. Insights into the early liver stage biology of *Plasmodium*. Journal of vector borne diseases. 2018;55(1):9-13.
33. Ménard R, Tavares J, Cockburn I, Markus M, Zavala F, Amino R. Looking under the skin: the first steps in malarial infection and immunity. Nature reviews Microbiology. 2013;11(10):701-12.
34. Prudêncio M, Rodriguez A, Mota MM. The silent path to thousands of merozoites: the *Plasmodium* liver stage. Nature reviews Microbiology. 2006;4(11):849-56.
35. Coppi A, Natarajan R, Pradel G, Bennett BL, James ER, Roggero MA, et al. The malaria circumsporozoite protein has two functional domains, each with distinct roles as sporozoites journey from mosquito to mammalian host. The Journal of experimental medicine. 2011;208(2):341-56.
36. Bowman NM, Congdon S, Mvalo T, Patel JC, Escamilla V, Emch M, et al. Comparative population structure of *Plasmodium falciparum* circumsporozoite protein NANP repeat lengths in Lilongwe, Malawi. Scientific reports. 2013;3:1990.
37. Ghasparian A, Moehle K, Linden A, Robinson JA. Crystal structure of an NPNA-repeat motif from the circumsporozoite protein of the malaria parasite *Plasmodium falciparum*. Chemical Communications. 2006(2):174-6.
38. Plassmeyer ML, Reiter K, Shimp RL, Jr., Kotova S, Smith PD, Hurt DE, et al. Structure of the *Plasmodium falciparum* circumsporozoite protein, a leading malaria vaccine candidate. J Biol Chem. 2009;284(39):26951-63.
39. Doud MB, Koksal AC, Mi LZ, Song G, Lu C, Springer TA. Unexpected fold in the circumsporozoite protein target of malaria vaccines. Proceedings of the National Academy of Sciences of the United States of America. 2012;109(20):7817-22.

40. Guy AJ, Irani V, MacRaild CA, Anders RF, Norton RS, Beeson JG, et al. Insights into the Immunological Properties of Intrinsically Disordered Malaria Proteins Using Proteome Scale Predictions. PloS one. 2015;10(10):e0141729.
41. Chaudhury S, MacGill RS, Early AM, Bolton JS, King CR, Locke E, et al. Breadth of humoral immune responses to the C-terminus of the circumsporozoite protein is associated with protective efficacy induced by the RTS,S malaria vaccine. 2020:2020.11.15.20232033.
42. Ainavarapu SRK, Patra A, Sharma S. Force Spectroscopy of the *Plasmodium falciparum* Vaccine Candidate Circumsporozoite Protein Suggests a Mechanically Pliable Repeat Region. Journal of Biological Chemistry. 2016;292.
43. Espinosa DA, Gutierrez GM, Rojas-López M, Noe AR, Shi L, Tse S-W, et al. Proteolytic Cleavage of the *Plasmodium falciparum* Circumsporozoite Protein Is a Target of Protective Antibodies. The Journal of infectious diseases. 2015;212(7):1111-9.
44. Aly AS, Vaughan AM, Kappe SH. Malaria parasite development in the mosquito and infection of the mammalian host. Annual review of microbiology. 2009;63:195-221.
45. Aliprandini E, Tavares J, Panatieri RH, Thiberge S, Yamamoto MM, Silvie O, et al. Cytotoxic anti-circumsporozoite antibodies target malaria sporozoites in the host skin. Nature microbiology. 2018;3(11):1224-33.
46. Julien J-P, Wardemann H. Antibodies against *Plasmodium falciparum* malaria at the molecular level. Nature Reviews Immunology. 2019;19(12):761-75.
47. Coppi A, Tewari R, Bishop JR, Bennett BL, Lawrence R, Esko JD, et al. Heparan sulfate proteoglycans provide a signal to *Plasmodium* sporozoites to stop migrating and productively invade host cells. Cell host & microbe. 2007;2(5):316-27.
48. Pinzon-Ortiz C, Friedman J, Esko J, Sinnis P. The binding of the circumsporozoite protein to cell surface heparan sulfate proteoglycans is required for *plasmodium* sporozoite attachment to target cells. The Journal of biological chemistry. 2001;276(29):26784-91.
49. Wardemann H, Murugan R. From human antibody structure and function towards the design of a novel *Plasmodium falciparum* circumsporozoite protein malaria vaccine. Current opinion in immunology. 2018;53:119-23.
50. Hügel FU, Pradel G, Frevert U. Release of malaria circumsporozoite protein into the host cell cytoplasm and interaction with ribosomes. Molecular and biochemical parasitology. 1996;81(2):151-70.
51. van de Sand C, Horstmann S, Schmidt A, Sturm A, Bolte S, Krueger A, et al. The liver stage of *Plasmodium berghei* inhibits host cell apoptosis. Molecular microbiology. 2005;58(3):731-42.
52. Maier AG, Cooke BM, Cowman AF, Tilley L. Malaria parasite proteins that remodel the host erythrocyte. Nature reviews Microbiology. 2009;7(5):341-54.
53. Marti M, Good RT, Rug M, Knuepfer E, Cowman AF. Targeting malaria virulence and remodeling proteins to the host erythrocyte. Science (New York, NY). 2004;306(5703):1930-3.
54. Hiller NL, Bhattacharjee S, van Ooij C, Liolios K, Harrison T, Lopez-Estraño C, et al. A host-targeting signal in virulence proteins reveals a secretome in malarial infection. Science (New York, NY). 2004;306(5703):1934-7.
55. de Koning-Ward TF, Gilson PR, Boddey JA, Rug M, Smith BJ, Papenfuss AT, et al. A newly discovered protein export machine in malaria parasites. Nature. 2009;459(7249):945-9.
56. Elsworth B, Matthews K, Nie CQ, Kalanon M, Charnaud SC, Sanders PR, et al. PTEX is an essential nexus for protein export in malaria parasites. Nature. 2014;511(7511):587-91.
57. Beck JR, Muralidharan V, Oksman A, Goldberg DE. PTEX component HSP101 mediates export of diverse malaria effectors into host erythrocytes. Nature. 2014;511(7511):592-5.
58. Deng XF, Zhou D, Liu QX, Zheng H, Ding Y, Xu WY, et al. *Plasmodium* circumsporozoite protein suppresses the growth of A549 cells via inhibiting nuclear transcription factor κB. Oncology letters. 2018;15(5):6585-91.
59. Oyen D, Torres JL, Wille-Reece U, Ockenhouse CF, Emerling D, Glanville J, et al. Structural basis for antibody recognition of the NANP repeats in *Plasmodium falciparum* circumsporozoite protein. Proceedings of the National Academy of Sciences of the United States of America. 2017;114(48):E10438-e45.

60. Diesbach P, N'Kuli F, Delmée M, Courtoy PJ. Infection by *Mycoplasma hyorhinis* strongly enhances uptake of antisense oligonucleotides: a reassessment of receptor-mediated endocytosis in the HepG2 cell line. Nucleic acids research. 2003;31:886-92.
61. Tompa P. Intrinsically unstructured proteins. Trends in biochemical sciences. 2002;27(10):527-33.
62. Noe AR, Espinosa D, Li X, Coelho-Dos-Reis JGA, Funakoshi R, Giardina S, et al. A full-length *Plasmodium falciparum* recombinant circumsporozoite protein expressed by *Pseudomonas fluorescens* platform as a malaria vaccine candidate. PloS one. 2014;9(9):e107764-e.
63. Thermo Fisher Scientific. Overview of Protein–Protein Interaction AnalysisOverview of Protein–Protein Interaction Analysis: Thermo Fisher Scientific; [cited 2021 05 june]. Available from: https://www.thermofisher.com/be/en/home/life-science/protein-biology/protein-biology-learning-center/protein-biology-resource-library/pierce-protein-methods/overview-protein-protein-interaction-analysis.html.

APPENDIX

SUPPLEMENTARY MATERIALS

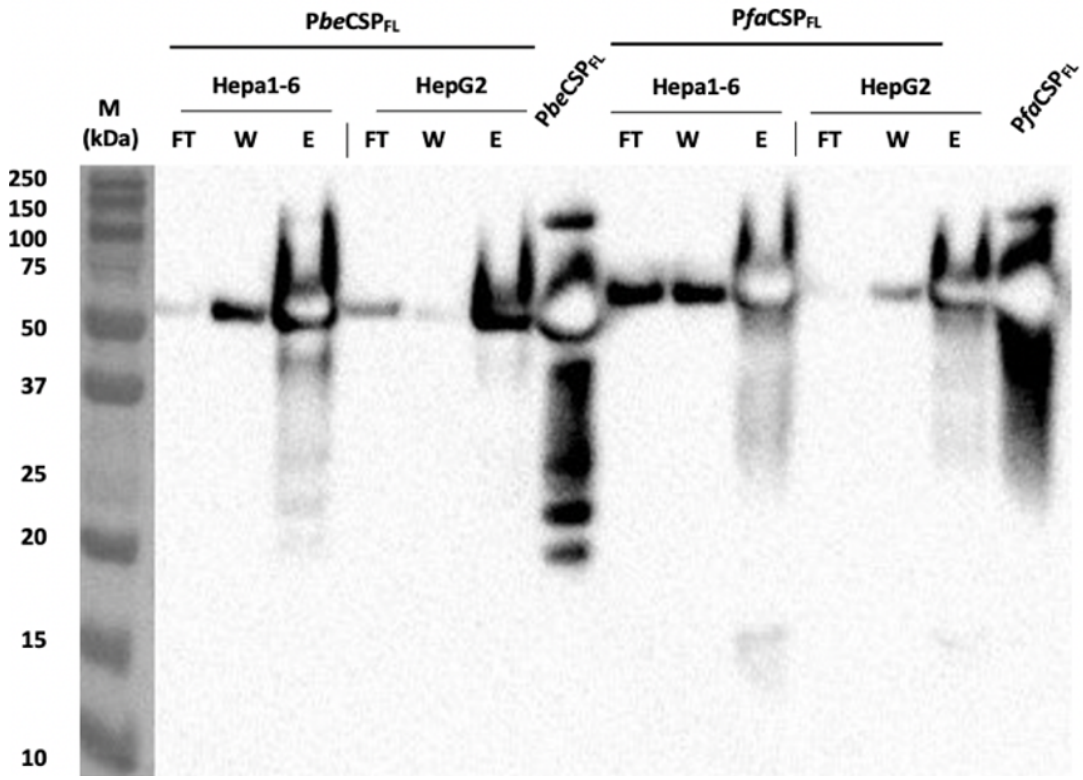

Supplementary figure S1 **FIRST ROUND OF PULL-DOWN ASSAYS**. Anti-importin-α western blot. Abbreviations: M = reference marker, FT = flow-through, W = wash, E = elution.

Supplementary table S1 **THE SEQUENCE IDENTITY OF HUMAN AND MOUSE IMPORTIN-α*3* PROTEINS.** (Sequences reprinted from UniProt: O35343 and O00629)

IMPORTIN SUBUNIT α-3	
Homo sapiens (human)	*Mus musculus* (mouse)
AMINO ACID SEQUENCES	
MADNEKLDNQRLKNFKNKGRDLETMRRQ RNEVVVELRKNKRDEHLLKRRNVPHEDIC EDSDIDGDYRVQNTSLEAIVQNASSDNQGI QLSAVQAARKLLSSDRNPPIDDLIKSGILPIL VHCLERDDNPSLQFEAAWALTNIASGTSE QTQAVVQSNAVPLFLRLLHSPHQNVCEQA VWALGNIIGDGPQCRDYVISLGVVKPLLSF ISPSIPITFLRNVTWVMVNLCRHKDPPPPME TIQEILPALCVLIHHTDVNILVDTVWALSYL TDAGNEQIQMVIDSGIVPHLVPLLSHQEVK VQTAALRAVGNIVTGTDEQTQVVLNCDAL SHFPALLTHPKEKINKEAVWFLSNITAGNQ QQVQAVIDANLVPMIIHLLDKGDFGTQKE AAWAISNLTISGRKDQVAYLIQQNVIPPFC NLLTVKDAQVVQVVLDGLSNILKMAEDE AETIGNLIEECGGLEKIEQLQNHENEDIYKL AYEIIDQFFSSDDIDEDPSLVPEAIQGGTFGF NSSANVPTEGFQF	MADNEKLDNQRLKNFKNKGRDLETMRRQ RNEVVVELRKNKRDEHLLKRRNVPQEDIC EDSDIDGDYRVQNTSLEAIVQNASSDNQGI QLSAVQAARKLLSSDRNPPIDDLIKSGILPIL VHCLERDDNPSLQFEAAWALTNIASGTSE QTQAVVQSNAVPLFLRLLHSPHQNVCEQA VWALGNIIGDGPQCRDYVISLGVVKPLLSF ISPSIPITFLRNVTWVMVNLCRHKDPPPPME TIQEILPALCVLIHHTDVNILVDTVWALSYL TDAGNEQIQMVIDSGIVPHLVPLLSHQEVK VQTAALRAVGNIVTGTDEQTQVVLNCDAL SHFPALLTHPKEKINKEAVWFLSNITAGNQ QQVQAVIDANLVPMIIHLLDKGDFGTQKE AAWAISNLTISGRKDQVAYLIQQNVIPPFC NLLTVKDAQVVQVVLDGLSNILKMAEDQ AETIANLIEECGGLEKIEQLQNHENEDIYKL AYEIIDQFFSSDDIDEDPSLVPESVQGGTFG FNSSTNVPTEGFQF
SEQUENCE SIMILARITY	
98.8% identity in 521 residues overlap	

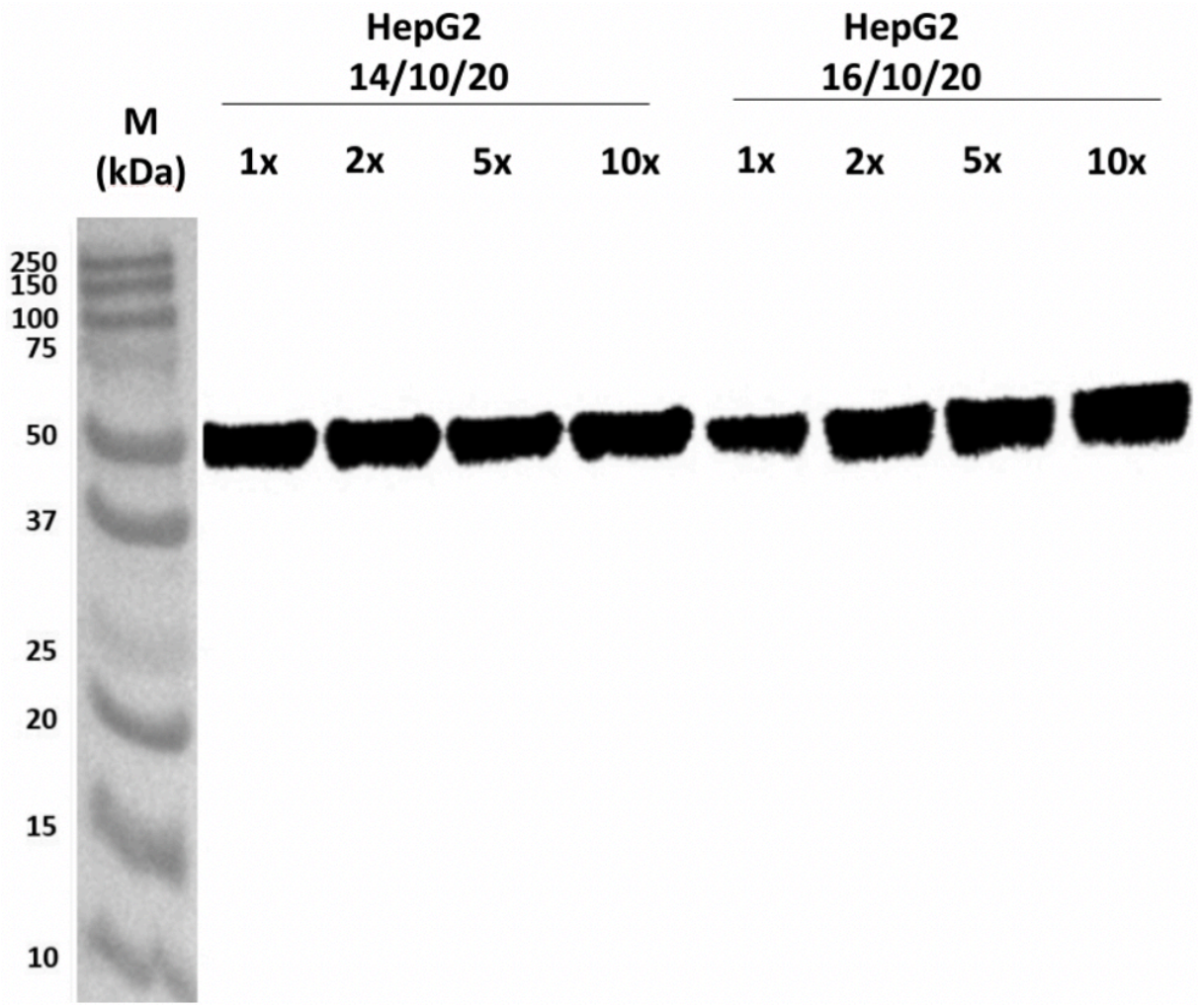

Supplementary figure S2 **IMPORTIN-α PROTEINS ARE DETECTED IN HEPG2 LYSATES.** Abbreviation: M = reference marker.

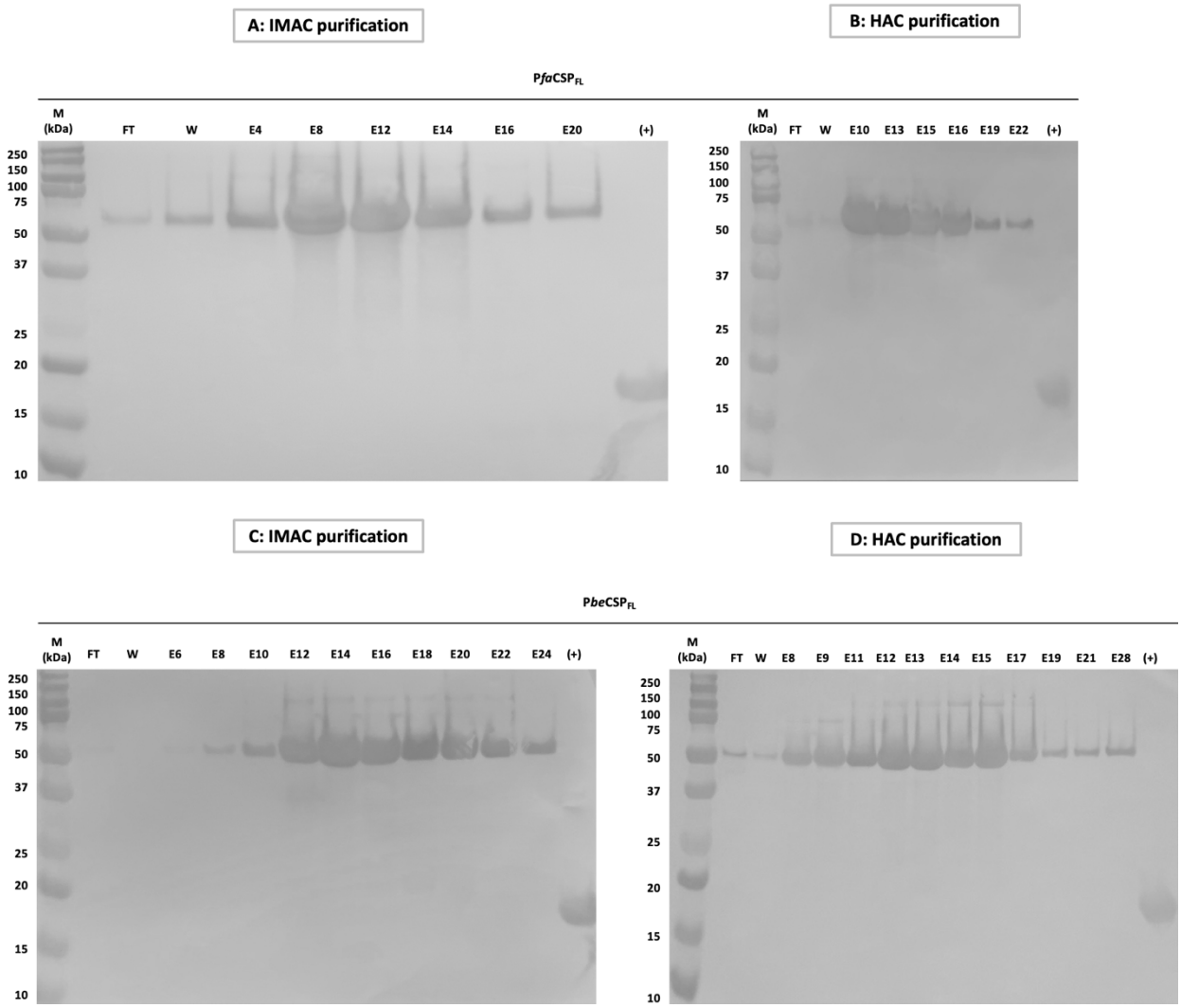

Supplementary figure S3 **PURIFICATION OF CSP**. (A) IMAC purification: anti-His WB (*Pfa*CSP$_{FL}$). (B) HAC purification: anti-His WB (*Pfa*CSP$_{FL}$). (C) IMAC purification: anti-His WB (*Pbe*CSP$_{FL}$). (D) HAC purification: anti-His WB (*Pbe*CSP$_{FL}$). Abbreviations: M = reference marker, FT = flow-through, W = wash, E = elution, (+) = positive control.

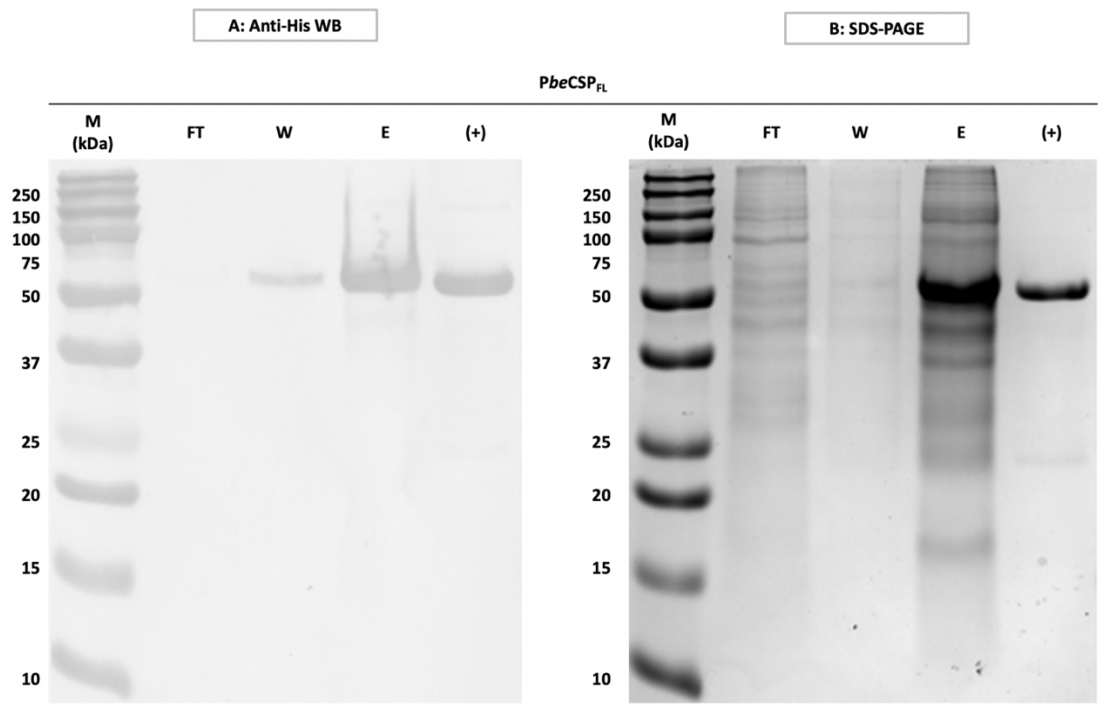

Supplementary figure S4 **THE SECOND PULL-DOWN ASSAY WITH *Pbe*CSP$_{FL}$**. (A) Anti-His WB. (B) SDS-PAGE with CBB staining. Abbreviations: M = reference marker, FT = flow-through, W = wash, E = elution, (+) = positive control.

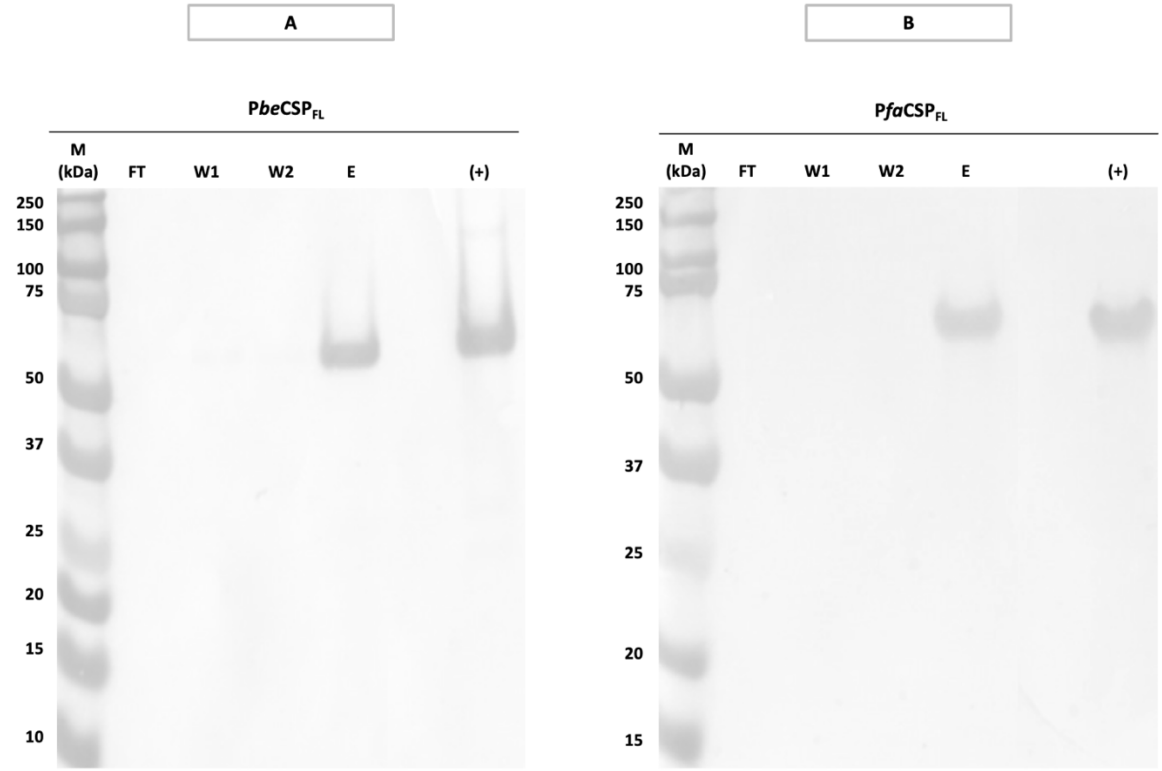

Supplementary figure S5 **THE THIRD PULL-DOWN ASSAY.** (A) *Pbe*CSP$_{FL}$: anti-His WB. (B) *Pfa*CSP$_{FL}$: anti-His WB. Abbreviations: M = reference marker, FT = flow-through, W = wash, E = elution, (+) = positive control.